Journal of Volcanology and Geothermal Research 187 (2009) 33–52

Contents lists available at ScienceDirect

Journal of Volcanology and Geothermal Research

journal homepage: www.elsevier.com/locate/jvolgeores

Syn-extensional intra-plate trachydacite-rhyolitic dome volcanism of the Mesa Central, southern Sierra Madre Occidental volcanic province, Mexico

A. Aguillón-Robles [a,*], M. Tristán-González [a], G.J. Aguirre-Díaz [b], H. Bellon [c]

[a] Instituto de Geología/DES Ingeniería, Universidad Autónoma de San Luis Potosí, San Luis Potosí, México
[b] Centro de Geociencias, Universidad Nacional Autónoma de México, UNAM, Campus Juriquilla, Querétaro, Querétaro, México
[c] UMR 6538, Domaines Océaniques, IUEM, Université de Bretagne Occidental, Brest, France

ARTICLE INFO

Article history:
Received 31 March 2009
Accepted 30 August 2009
Available online 9 September 2009

Keywords:
lava dome
tectono-magmatism
rhyolite–trachydacite
Sierra Madre Occidental
Mesa Central Mexico

ABSTRACT

Oligocene dome complexes of trachydacitic to rhyolitic composition are common in the southern portion of the Mesa Central physiographic province, which forms part of the southern Basin and Range extensional province as well as of the southern Sierra Madre Occidental volcanic province. Generally, dome complexes occur aligned with regional fault systems, mostly associated with the southern Basin and Range province, and thus suggesting that faults controlled the felsic magmas that formed these domes. Two distribution patterns are evident, one aligned NE–SW and another aligned NNE. The set of domes were emplaced at 33–28 Ma. Emplacement of domes occurred in three continuous phases starting with those of trachydacite affinity at 33–32 Ma, to trachydacite–rhyolitic at 32–31 Ma, and finally to those with rhyolitic composition at 31–28 Ma. Felsic magmas that originated the domes were apparently generated by partial melting at the base of the continental crust. Contrary to previous hypothesis, our evidence suggest that these magmas in these particular areas of the Mesa Central were not accumulated in large magma reservoirs emplaced at shallow levels in the crust, but crossed the continental crust directly. Since continental crust in this region is relatively thin (30–33 km), we propose that an intense extensional episode favored the direct ascension of these magmas through the brittle crust, with little interaction with the country rock during ascent to the surface, to end up forming aligned dome chains or complexes. Geochemical data favors this model, as the felsic rocks show no depletions in Nb and Th but instead relatively enrichment in these elements. REE show flat or concave up patterns, suggesting that the magmas involved enriched (fertile), metasomatized lithospheric fluids that generated partial melting at the base of the continental crust. Based upon these data, we infer an intra-plate tectonic setting for these rocks.

1. Introduction

During Oligocene, felsic volcanism was intense and widespread in the Sierra Madre Occidental (SMO) in western Mexico (McDowell and Clabaugh, 1979; Swanson and McDowell, 1984; Aguirre-Díaz and Labarthe-Hernández, 2003). Felsic rocks of the SMO have been classified within the K-rich calc-alkaline suite (McDowell and Clabaugh, 1979; Cameron et al., 1980; Aranda-Gómez et al., 1983). Most of this volcanism was explosive and has been referred to as the Ignimbrite Flare-up (McDowell et al., 1990; Aguirre-Díaz and McDowell, 1991; Ferrari et al., 2002; Aguirre-Díaz et al., 2008). However, part of this mid-Tertiary volcanism was effusive, particularly, in the southern Mesa Central, where 80 vol.% of middle Oligocene felsic magmatism is represented by lava domes and only 20 vol.% by ignimbrites. Some of these domes are associated with hydrothermal mineralization that formed important precious metal deposits throughout the SMO (Burt et al., 1982; Huspeni et al., 1984; Scheubell et al., 1988; Webster et al., 1996), Sn deposits (Foshag and Fries, 1942; Lee-Moreno, 1972), and topaz-bearing rhyolites (Burt et al., 1982; Burt and Sheridan, 1987).

In general, lava domes can be emplaced at distinct tectono-magmatic regimes (Fink, 1987). Sometimes domes are related to post-collapse activity in calderas (Lipman, 1984; Henry and Price, 1984; Aguirre-Díaz et al., 2007, 2008), and in other cases lava domes are associated with faulting and extensional tectonic settings; these domes commonly bear Sn and topaz, such as those of SW United States (Christiansen et al., 1986). In the southern SMO, near the city of San Luis Potosí, Sn and topaz-bearing lava domes were emplaced during the Oligocene (Tristán-González, 1986; Labarthe-Hernández and Tristán-González, 1988; Aranda-Gómez et al., 1989). These domes have been related with extensional tectonics since they occur aligned with regional fault systems, either along graben or half-graben margins or inside them (Tristán-González, 1986; Nieto-Samaniego et al., 1996; Aranda-Gómez et al., 2000; Tristán-González et al., 2006, 2009a,b). Orozco-Esquivel et al. (2002) have proposed that these

* Corresponding author. Av. Dr. Manuel Nava # 5, Zona Universitaria, San Luis Potosí, S.L.P., México, C.P. 78250, México. Tel.: +52 444 817 1039; fax: +52 444 811 8321.
E-mail addresses: aaguillonr@uaslp.mx (A. Aguillón-Robles), ger@geociencias.unam.mx (G.J. Aguirre-Díaz), Herve.Bellon@univ-brest.fr (H. Bellon).

0377-0273/$ – see front matter © 2009 Elsevier B.V. All rights reserved.
doi:10.1016/j.jvolgeores.2009.08.021

Table 1
K–Ar isotopic ages.

Volcanic complex	Sample number	Coordinates		Age $\pm 1\sigma$	^{40}Ar[a] (e^{-7} cm^3)	% ^{40}Ar[a]	K_2O (wt.%)	Fraction[a]	Analyzed weight (g)	Ref.[b] analysis
		Latitude N	Longitude W							
SLPVF[1]	SLP00-19			27.4 ± 0.4				fds		
SIC	SLP00-16	21°55′53.5″	101°53′03.3″	28.5 ± 0.5	47.7	74.3	5.15	fds	0.3000	B5578
OC	SLP03-07	21°49′48.5″	101°41′49.5″	28.7 ± 0.7	50.7	75.5	5.45	wr	0.3475	B7078
SLPVF[2]	SLP00-03			28.9 ± 0.5				wr		
AMC	SLP00-13	22°13′51.9″	96°06′32.1″	29.5 ± 0.5	58.8	78.4	6.13	fds	0.2511	B5526
AMC	SLP00-10	23°01′23.4″	101°51″06.8″	30.3 ± 0.5	24.4	82.3	2.48	fds	0.4037	B5555
SLPVF[3]	SLP00-17			30.4 ± 0.5				fds		
SIC	SLP06-07	101°45′23.5″	21°42′26.7″	30.4 ± 0.7	53.6	81.2	5.43	wr	0.3593	B7067
SLPVF[4]	SLP01-22			31.0 ± 0.7				mtx		
AMC	SLP00-09	23°03′37.7″	101°53′41.5″	31.2 ± 0.5	46.8	90.5	4.61	fds	0.2511	B5554
OC	SLP01-07	21°50′49.2″	101°39′05.9″	31.5 ± 0.7	56.1	85.3	5.48	wr	0.3596	B7068
SLPVF[5]	JAG37-03			31.6 ± 0.7				wr		
SLPVF[6]	SLP01-21			31.6 ± 0.8				wr		
AMC	SLP00-15	22°08′48.0″	101°58′01.6″	32.3 ± 0.5	56.1	95.2	5.35	fds	0.3024	B5585
EPC	SLP00-11	21°36′06.3″	101°22′18.1″	32.9 ± 0.6	30.2	59.0	2.82	fds	0.4023	B5556
SIC	SLP00-12	21°28′06.7″	96°00′24.9″	33.3 ± 0.5	53.2	86.8	4.91	fds	0.2615	B5557

All are new ages except for the samples SLPVF reported by Tristán-González et al. (2009a,b).
[1]Trz; El Zapote rhyolite; [2]Trp; Panalillo ignimbrite; [3]Tsm; San Miguelito rhyolite; [4]Tlp; Portezuelo dacite; [5]Toc; Ojo Caliente trachyte; [6]Tdj; Jacavaquero dacite.
[a] Used material; fds — feldspar; wr — whole rock; mtx — matrix.
[b] Laboratory reference of the analyses performed in the Geochronology Laboratory at the Université de Bretagne Occidentale, Brest, France.

felsic lavas result from partial melting of Precambrian continental crust, in a similar way as have been suggested for the topaz rhyolites in the SW United States (Christiansen and Lipman, 1966; Christiansen et al., 1984, 1986). Verma (1984) already has proposed this hypothesis for domes of the southern SMO mentioning that partial melting probably took place at the base of continental crust. Rodríguez-Ríos et al. (2007) in a more recent study agree with the continental crust anatexis model, but include a minor percent of crystal fractionation in the evolution processes.

In order to better understand the origin of this voluminous felsic pulse during Oligocene, we combined geochemical data with well-constrained geological, stratigraphical and geochronological data,

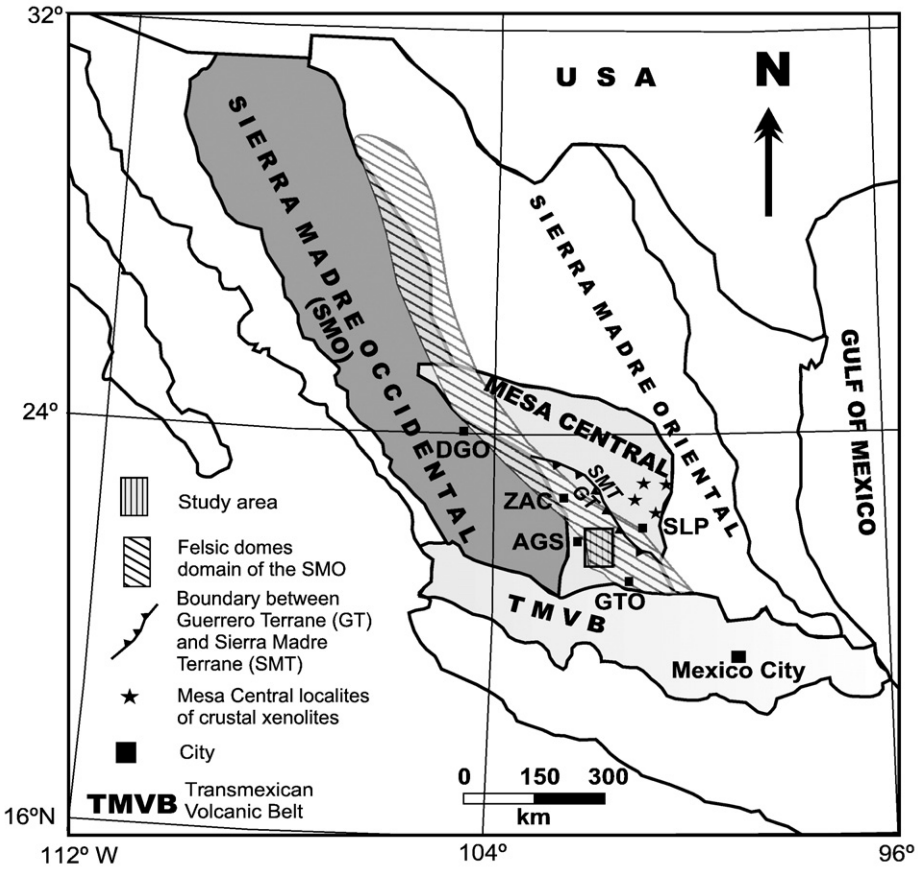

Fig. 1. Index map showing the location of the study area and the geologic provinces of Sierra Madre Occidental, Sierra Madre Oriental, Mesa Central, and Transmexican Volcanic Belt. Also indicated is the extent of the felsic domes domain at the eastern Sierra Madre Occidental. Outlined are the boundaries of Sierra Madre (SMT) and Guerrero (GT) terranes. Towns: AGS — Aguascalientes, DGO — Durango, GTO — Guanajuato, SLP — San Luis Potosí, ZAC — Zacatecas.

most of which are the products of regional geologic maps drawn up in the past years (Labarthe-Hernández et al., 1982, 1989; Labarthe-Hernández and Jiménez-López, 1991, 1992; Labarthe-Hernández and Tristán-González, 1988; Tristán-González, 1986). New radiometric ages are included in this study (Table 1), which were needed to resolve some specific time constraints. All these combined data allows a better grasp about how the magmatic processes changed with time, and permits better constrains on the evolution of the tectono-magmatic processes involved in the generation and evolution of these magmas. Here we present major and trace geochemical information tied to this geological–stratigraphical and geochronological control. Our work describes four dome complexes, 1) El Pájaro, 2) Ojuelos, 3) Aguas Muertas, and 4) Santa Inés (Figs. 1 and 2), which represent the general nature of the felsic effusive Oligocene volcanism in the southern Mesa Central, and that particularly occurs in a zone of major extension and minimum crustal thickness with respect other areas of the Sierra Madre Occidental.

2. Regional geological and tectonic framework

2.1. Geological framework

The south-eastern portion of the SMO volcanic province includes an elevated plateau known as the Mesa Central that is limited to the east–northeast by the Mesozoic folded belt of Sierra Madre Oriental and to the west by the high ranges of Sierra Madre Occidental (Fig. 1). The Mesa Central concentrates several Oligocene volcanic fields of predominantly trachydacitic to rhyolitic lava domes, including San Luis Potosí, Santa María del Río, and Guanajuato, as well as others in the states of Aguascalientes, Jalisco and Zacatecas (Labarthe-Hernández et al., 1982; Tristán-González, 1986; Labarthe-Hernández et al., 1989; Aranda-Gómez et al., 1989; Labarthe-Hernández and Jiménez-López, 1991, 1992). The basement of this region is formed by volcano-sedimentary sequences of the Guerrero and Sierra Madre terranes (Campa and Coney, 1983). The Guerrero terrane is one of the largest

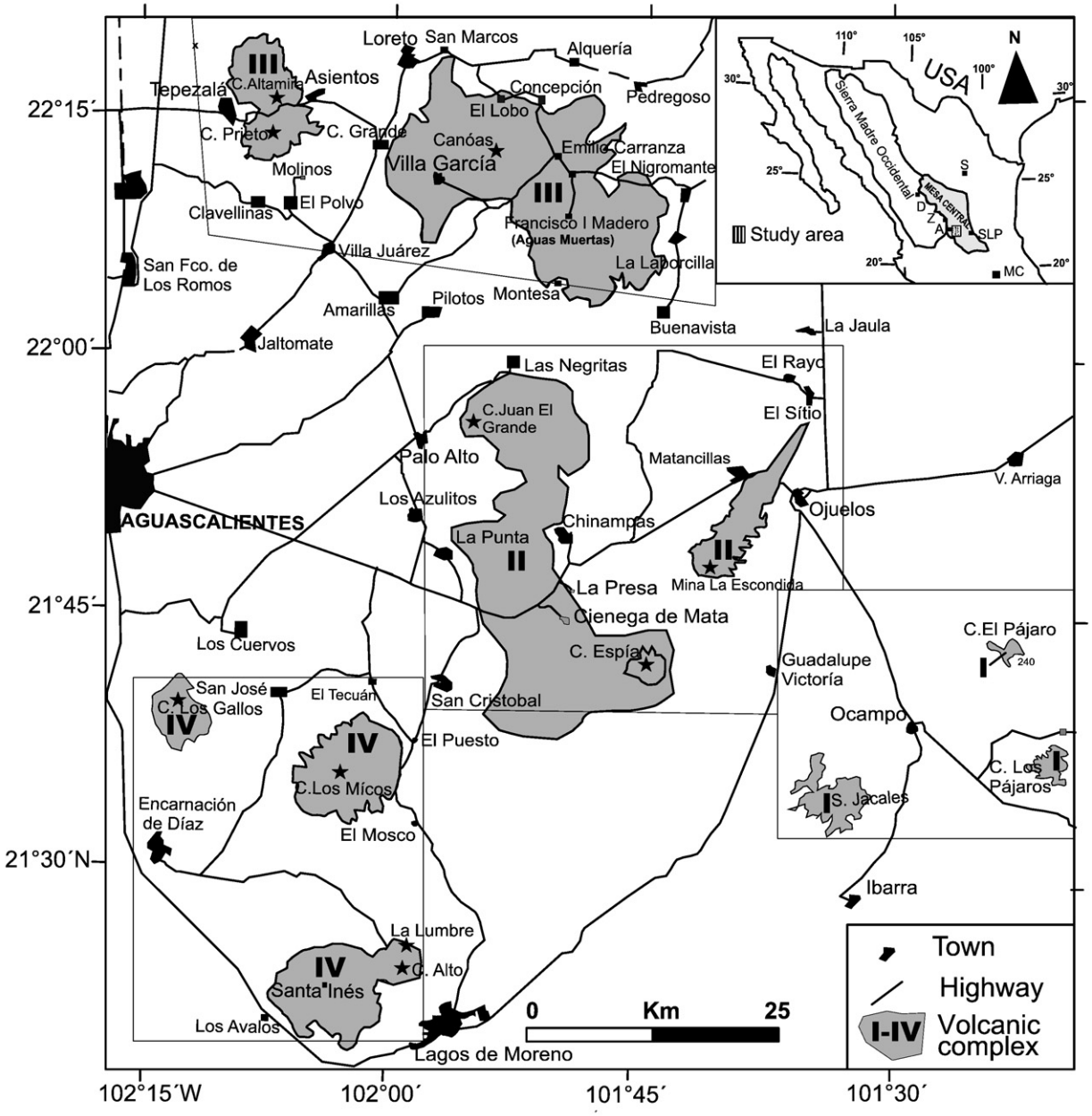

Fig. 2. Location of the 4 studied dome complexes in the southern Mesa Central. I — El Pájaro Complex, II — Ojuelos Complex, III — Aguas Muertas Complex, IV — Santa Inés Complex. Stars represent localities mentioned in text. Inset shows simplified regional index map. Cities: A — Aguascalientes, D — Durango, S — Saltillo, Z — Zacatecas, SLP — San Luis Potosí.

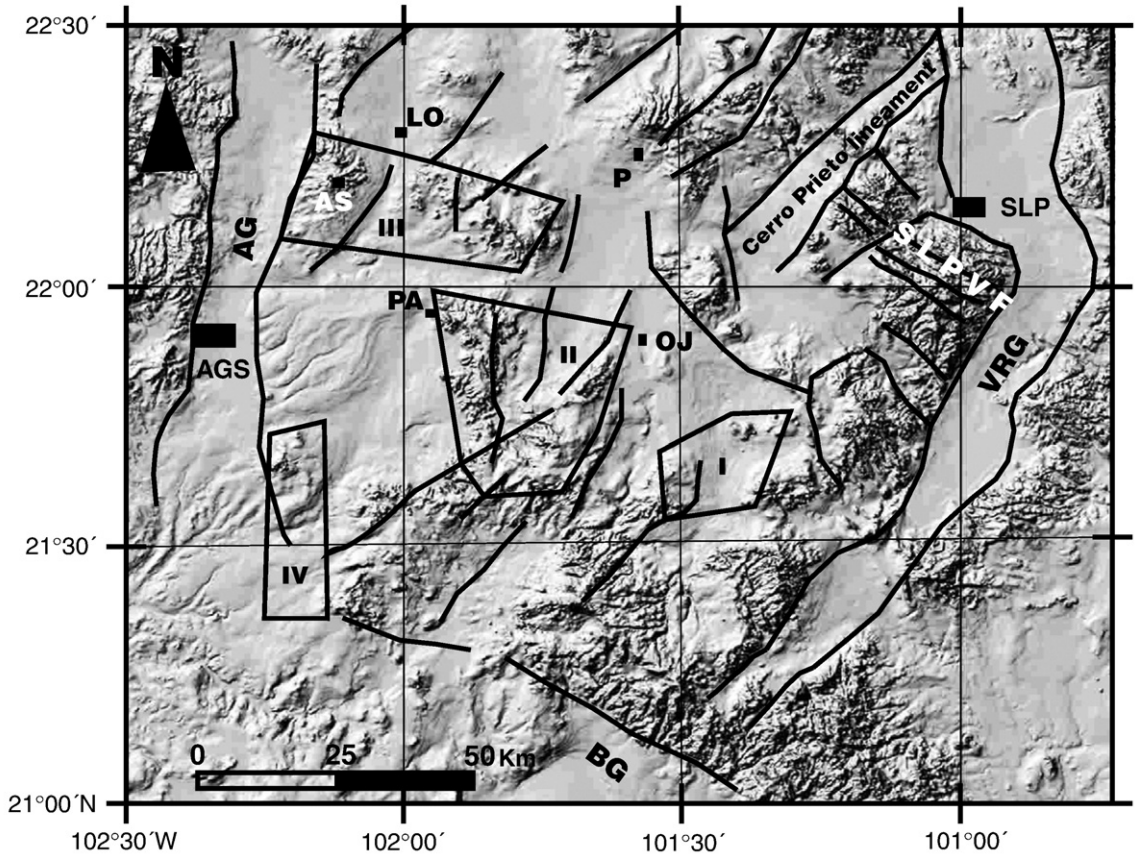

Fig. 3. Digital elevation model for the southern Mesa Central, including the dome complexes studied. Note the alignment of ranges formed by these complexes and the normal faults affecting the area. Numbering of complexes as in Fig. 2. Main structures are: VRG — Villa de Reyes graben, AG — Aguascalientes graben, BG — Bajio graben, SLPVF — San Luis Potosí volcanic field. Towns: LO — Loreto, OJ — Ojuelos, PA — Palo Alto, P — Pinos, AGS — Aguascalientes, SLP — San Luis Potosí, AS — Asientos.

accreted tectono-stratigraphic terranes of Mexico, and was accreted to North America craton at Late Cretaceous post-Cenomanian (Centeno-García et al., 1993). The Guerrero terrane sequence includes andesite, sandstone, shale and mafic lava dike complexes with Late Jurassic to Early Cretaceous ages (McGehee, 1976; Yta, 1992; Centeno-García et al., 1993). The Sierra Madre terrane consists of a folded Mesozoic marine sequence, mainly carbonates, which as deposited on the Mesozoic Basin of Central Mexico and the Valles–San Luis Potosí submarine platform (Carrillo-Bravo, 1971, 1982; López-Doncel, 2003). Most of the Oligocene felsic lavas at the Mesa Central cover older rocks of the SMO that belong to the Upper Volcanic Supergroup (McDowell and Clabaugh, 1979). This sequence is characterized by a thick package of felsic ignimbrites and lavas ranging in age from 38 to 23 Ma (Lee-Moreno, 1972; McDowell and Clabaugh, 1979; Cameron et al., 1980; Huspeni et al., 1984; Aguirre-Díaz and McDowell, 1991; Aguirre-Díaz et al., 2008).

On a regional scale, the felsic domes form an 800 km long discontinuous volcanic belt trending NW–SE along the eastern margin of the SMO, including the Mesa Central, (Fig. 1). The main characteristic of this belt is the abundance of Sn and Hg deposits. Huspeni et al. (1984) consequently called it the Mexican Tin Belt. These tin-rich domes have been related to the extensional tectonics of the Basin and Range during the Oligocene (Labarthe-Hernández et al., 1982; Tristán-González, 1986; Aguillón-Robles et al., 1994; Nieto-Samaniego et al., 1999; Tristán-González et al., 2005). Most of the domes were emplaced as discrete punctual structures along inferred NW–SE and NE–SW normal fault systems, forming in this way long chains of aligned lava domes. In some cases, rhyolitic lava dikes and domes with elongated shapes also occur within these alignments. Burt and Sheridan (1987) studied some of these domes in the states of Guanajuato and San Luis Potosí and they classified them as topaz rhyolites mentioning the great similarity with the mid-Tertiary topaz rhyolites of the SW United States. The U.S. rhyolites have been explained as formed by anatexis of Precambrian continental crust (Christiansen et al., 1986; Ruiz et al., 1988, 1990). In the Mesa Central there are no outcrops of Precambrian rocks, but there is evidence of Precambrian crust in this area from crustal xenoliths in Quaternary basalts (Fig. 1; Schaaf et al., 1994; Aranda-Gómez et al., 2000). It must be mentioned that other areas of the SMO include felsic lava domes that postdate Eocene, Oligocene and Miocene large-volume ignimbrites, which are assumed to be related to shallow magma chambers that fed fissure type eruptions (Tristán-González, 1986; Aguirre-Díaz and Labarthe-Hernández, 2003; Tristán-González et al., 2006). The domes described here do not form part of that other suite of domes, which are generally related to graben-caldera post-collapse effusive volcanism (Aguirre-Díaz et al., 2008).

2.2. Tectonic framework

The Oligocene trachydacite to rhyolitic dome complexes were emplaced on top of a crust about 30–33 km thick (Meyer et al., 1958; Fix, 1975; Smith and Jones, 1979; Rivera and Ponce, 1986) that includes a) Precambrian crystalline lower crust, b) Mesozoic Sierra Madre and Guerrero terranes, c) Lower to Upper Cretaceous volcano-marine sedimentary rocks, and d) the mid-Tertiary volcanic succession of the SMO (Burt and Sheridan, 1987; Ruiz et al., 1988; Henry and Aranda-Gómez, 1992; Centeno-García and Silva-Romo, 1997; Dickinson and Lawton, 2001; Nieto-Samaniego et al., 2005). The Guerrero terrane was accreted over the Sierra Madre terrane during the Middle to Upper Jurassic time (Centeno-García and Silva-Romo, 1997). Then,

at Late Cretaceous to Early Paleocene, Laramide orogeny folded and thrusted these older rocks as well as the Cretaceous platform marine rocks in a NE compression direction (De Cserna, 1956; Tardy et al., 1975; Padilla y Sánchez, 1985; Tristán-González, 2008). In the Late Paleocene–Early Eocene the region was affected by right-lateral transtension, and from Eocene to Miocene, by extension that occurred as several episodic events (Tristán-González et al., 2009a,b). Associated with this extension are several sets of normal faults, whose main orientation is NW–SE. They have been related with the Basin and Range regional event (Stewart, 1978; Henry and Aranda-Gómez, 1992; Tristán-González et al., 2009a,b). At early Oligocene, an intense episode of Basin and Range normal faulting occurred synchronously with felsic volcanism, either effusively as lava domes or explosively as ignimbrite-forming eruptions (Labarthe-Hernández et al., 1982; Tristán-González, 1986; Aguirre-Díaz and Labarthe-Hernández, 2003; Torres-Hernández et al., 2006; Tristán-González, 2008; Tristán-González et al., 2009a,b). Normal faulting continued after this volcanism and, at about 28–26 Ma, took place another Basin and Range episode that caused the maximum extension. During this peak extensional event a series of horsts, grabens and half-grabens were developed associated with eruption of ignimbrite-forming pyroclastic flows and basaltic andesites (Labarthe-Hernández et al., 1982; Tristán-González, 1986; Henry and Aranda-Gómez, 1992; Nieto-Samaniego et al., 1999; Aranda-Gómez et al., 2000; Nieto-Samaniego et al., 2005; Tristán-González et al., 2009a,b). Extension continued acting episodically at least until middle Miocene (Tristán-González et al., 2009a,b), and probably until Quaternary.

The volcanic dome complexes described in this study form in general aligned arrangements following the same orientation of the regional tectonic trends (Fig. 1, 3). The domes may occur either as elongated bodies extruded along the faults, or if long enough, as dikes, or as punctual centers aligned with the faults trends. Two main structural controls are observed, one trending NE–SW and parallel to the Villa de Reyes Graben, and another trending NNE and parallel to the Aguascalientes Graben (Fig. 3).

3. Geologic description of the lava dome complexes

3.1. El Pájaro dome complex

This dome complex is located in the SE portion of the study area. It is composed of several relatively small rhyolitic domes covering an area of about 700 km^2 (Fig. 2). The major structure is Los Jacales range that is an elliptical exogenous dome with an area of about 350 km^2. It

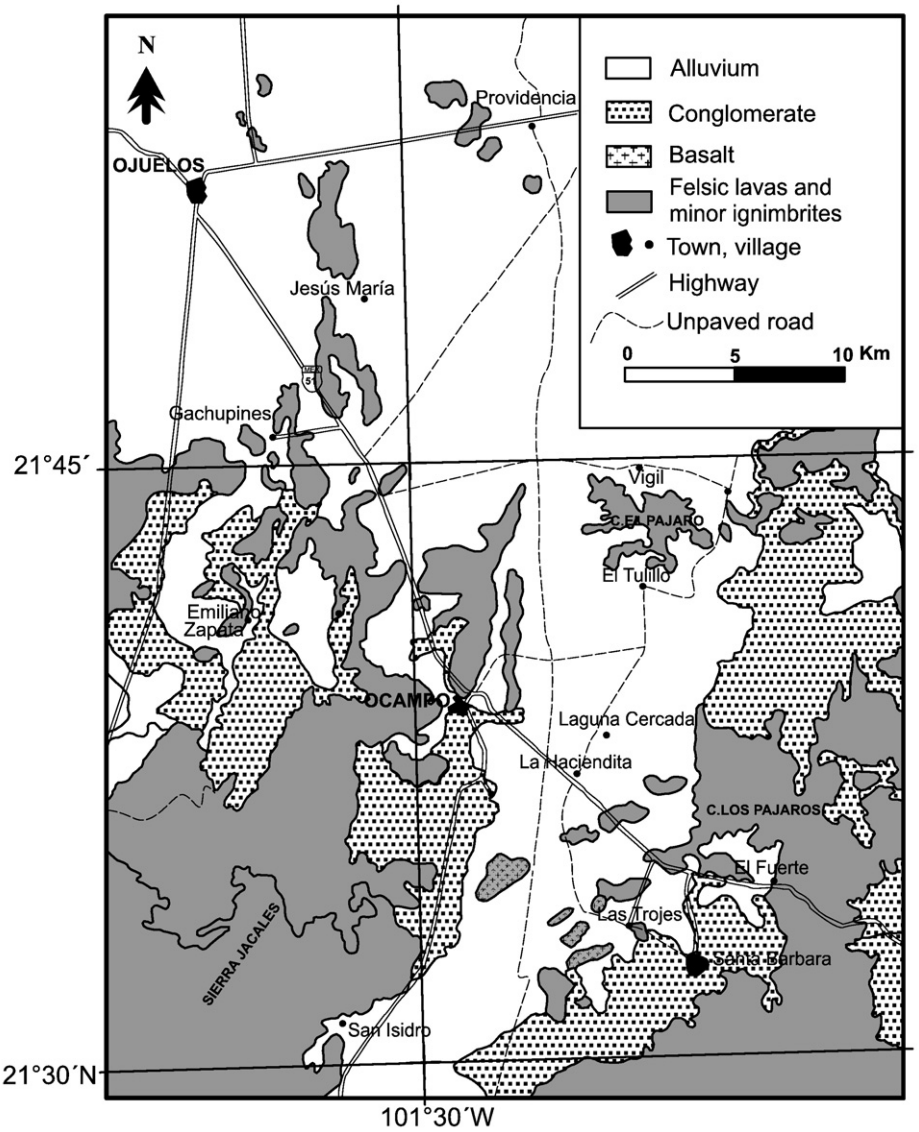

Fig. 4. Generalized geologic map of the El Pájaro dome complex.

is formed by several flow units organized with a radial arrangement from a central vent (Fig. 4). Two smaller domes, Los Pájaros and El Pájaro, as well as some other unnamed ones occur with elongated shapes aligned NS. The complex is made of several rhyolitic lavas showing flow banding, generally light pink, with 2–5 vol.% of phenocrysts, mainly sanidine and quartz (1–2 mm), and a devitrified matrix. Vent areas are usually silicified and with hydrothermal alteration. Vertical to semi-vertical flow foliation and breccia zones (auto-breccias) occur near to, or at the vent. The El Pájaro dome includes a pyroclastic sequence that precedes the lavas, consisting of lithics- and pumice-rich pyroclastic flow deposits, followed by a co-ignimbrite lithic breccia with lithics up to 20 cm in diameter, and an ashy matrix.

3.2. Ojuelos dome complex

The Ojuelos dome complex is the largest effusive structure. It is located in the central portion of the study area (Fig. 2). The main domes in this complex are Ojuelos, Palo Alto, Ciénega de Mata and El Espía (Fig. 5). In most cases, rhyolitic lavas were preceded by explosive phases that originated pyroclastic flow deposits. The domes and related pyroclastic rocks were emplaced on marine sedimentary rocks of the Guerrero terrane, which includes shales, sandstones and thin-bedded limestones, which in some cases occur interlayered with pillow lavas of intermediate composition (Fig. 6E). The sequence in Palo Alto (Fig. 5), measured at Cerro Juan El Grande, includes a sedimentary package of the Guerrero terrane, which is covered by a grey ignimbrite that varies from welded to unwelded ignimbrite with up to 3 vol.% of phenocrysts of sanidine and quartz, and small lithics and uncollapsed pumice in the unwelded zone, and then, rhyolitic lavas of the dome (Fig. 6B). The local stratigraphy for each dome of the Ojuelos complex is summarized in 6 representative measured sections shown in Fig. 6. Mingling of magmas is evident in this complex, with grey rhyolitic lavas intermingled with brown trachydacitic patches (Fig. 7).

3.3. Aguas Muertas dome complex

The Aguas Muertas dome complex lies in the SE portion of the State of Zacatecas and in the NE part of Aguascalientes State, covering an area of about 555 km^2 (Fig. 2). The southern part of this complex is formed by three large domes, Aguas Muertas, Canoas and Villa García (Fig. 8). The stratigraphy of this complex is shown in 4 measured sections in Fig. 9. Canoas locality includes two domes, an older one of

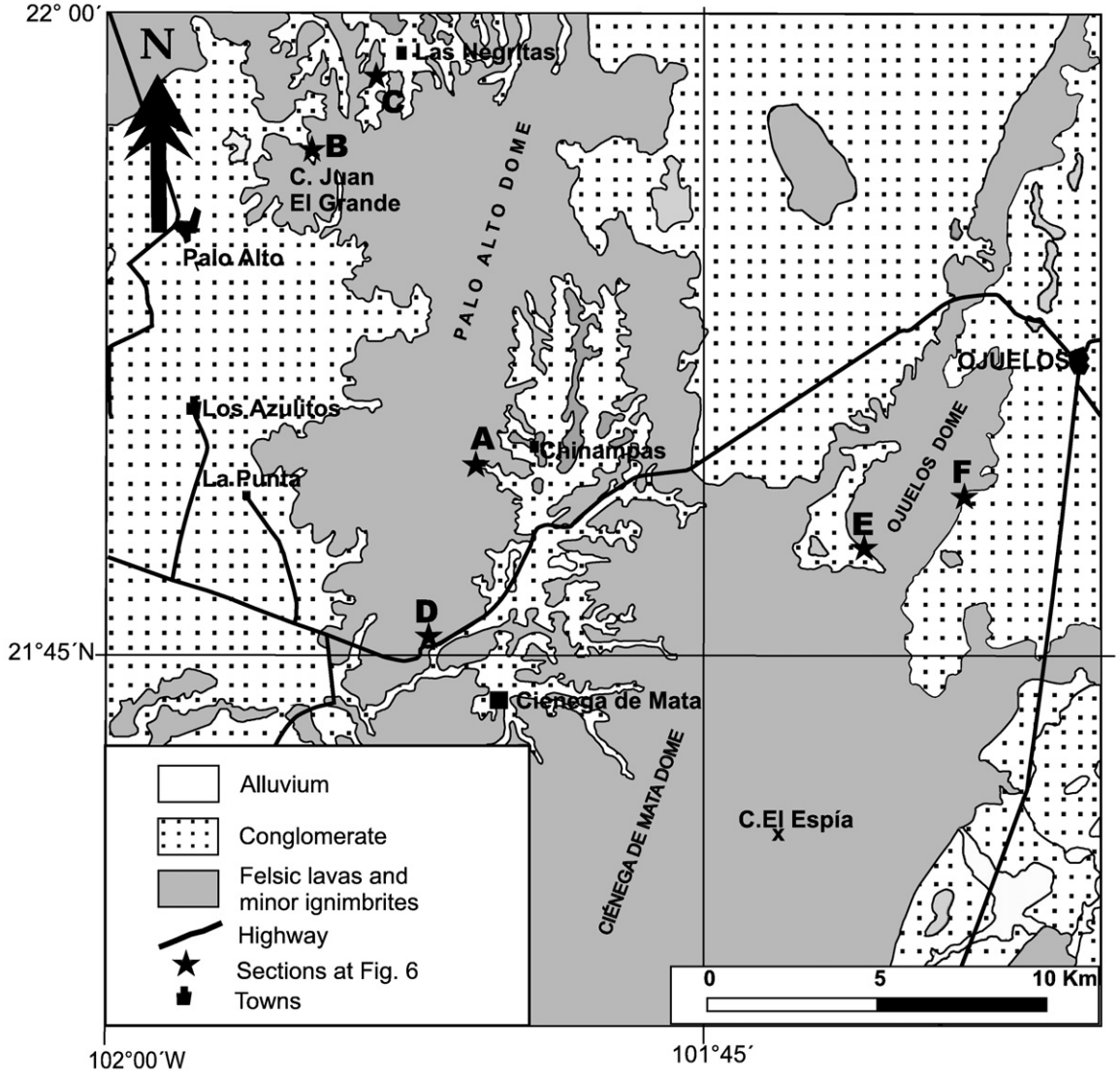

Fig. 5. Generalized geologic map of the Ojuelos dome complex.

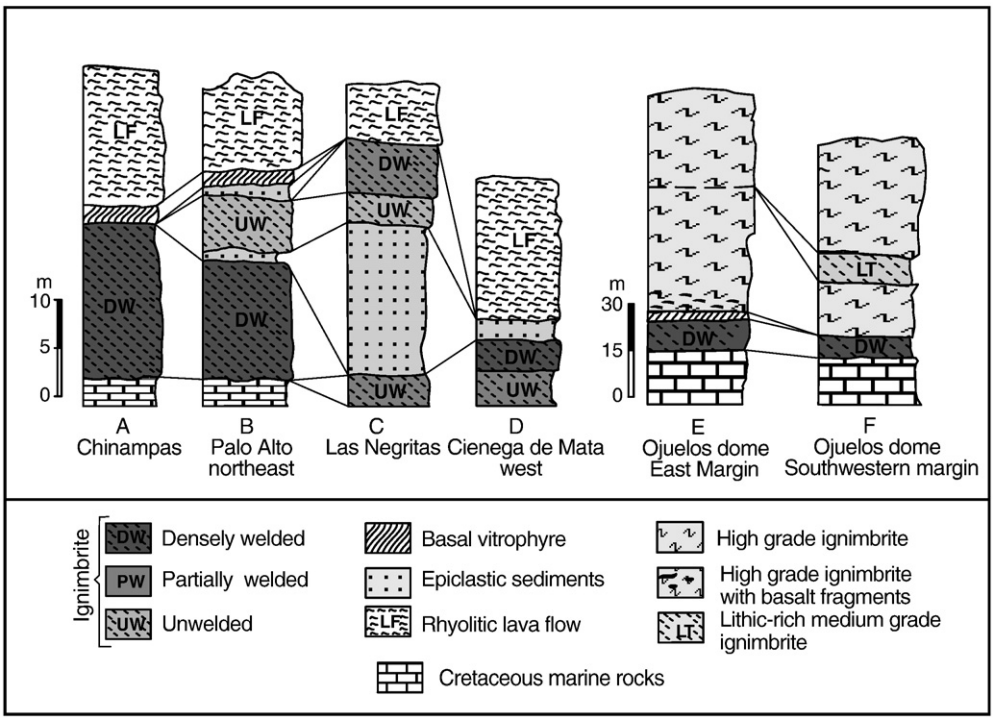

Fig. 6. Measured and correlation sections in the Ojuelos dome complex. The labels of the columns correspond to sections indicated in the map shown in Fig. 5.

trachydacitic composition and a younger one rhyolitic in composition (Fig. 9A). These domes cover Aptian reef-limestone (Tristán-González et al., 1994) and other type of marine sedimentary rocks that were folded during the Laramide orogeny (Fig. 9C and D). In general, in the Aguas Muertas complex, at the base of the domes there are reddish brown, welded ignimbrites, with 10 vol.% of phenocrysts of quartz and sanidine (Fig. 9A, B). Canoas was a very important mining district of Hg that exploited the dome carapace of dacitic composition. The lava is red, with 3–4 vol.% phenocrysts of plagioclase, sanidine and quartz in a reddish brown devitrified matrix with flow banding.

At the northern part of the complex is the Asientos–Tepezalá chain, which includes the Altamira, Los Pelones and El Prieto domes (Fig. 10). The Cerro Altamira (Fig. 11) is the vent from which several coulees were extruded and distributed mainly on the eastern flank. The lava at the Cerro Altamira vent zone is brown to gray, with a porphyritic texture and 3–5 vol.% of quartz and sanidine phenocrysts, as well as some altered Fe–Mg rich minerals; the matrix shows flow-banding and is devitrified. Several rhyolitic dikes with a NNE orientation outcrop to the south of the Cerro Altamira vent (Fig. 11). The dikes intruded Mesozoic marine sediments of Guerrero terrane, which are intensely silicified, oxidized and argilized. This hydrothermal alteration generated the ore deposits of the nearby El Orito mine that produces zinc, lead and silver. El Prieto dome is located to the SE of Cerro Altamira (Fig. 10). This dome is composed of porphyritic, brown lavas, with 3–5 vol.% of quartz and sanidine phenocrysts, 1–3 mm in size, and a devitrified matrix with flow banding.

Fig. 7. Field photograph showing the aspect of magma mingling in the Ojuelos dome complex lavas. The darker patches of the rock correspond to trachydacite lava and the rest to high-silica rhyolite lava.

3.4. Santa Inés dome complex

The Santa Inés complex includes the rhyolitic domes of Santa Inés, Micos–La Lumbre and Los Gallos (Fig. 12). Representative stratigraphic sections are shown in Fig. 13. The Santa Inés dome is located in the SE part of the complex. The volcanic sequence in this locality includes a trachydacitic, dark brown lava, with 20% vol. of plagioclase, sanidine, rare quartz phenocrysts, and a devitrified and fluidal matrix (Fig. 13B). Overlying this lava is a brown ignimbrite with 15–20 vol.% of sanidine and quartz phenocrysts, 2–3 mm in size, and a devitrified matrix. The ignimbrite is welded at the top and has a co-ignimbrite lithic lag breccia at the base. The ignimbrite is covered by the Santa Inés dome, a pink rhyolitic lava with a spherulitic base and 5 vol.% of quartz and sanidine phenocrysts of 2–3 mm in size, and a devitrified and fluidal matrix.

On the SW margin of the Santa Inés complex, to the east of Rancho Los Ávalos, the sequence includes rhyolitic lavas, with porphyritic texture, and 10 vol.% of quartz and sanidine phenocrysts, 2–3 mm diameter, in a devitrified and flow-banded matrix. Then, it is overlain by a 150 m thick ignimbrite package (Fig. 13A).

In the Cañada de La Lumbre, at the NE portion of Santa Inés complex is the central vent of the La Lumbre dome, named Cerro Alto (Fig. 12). The sequence consist from base to top of an ignimbrite with a basal surge, and then the lava dome flow, which is a brown gray rhyolite

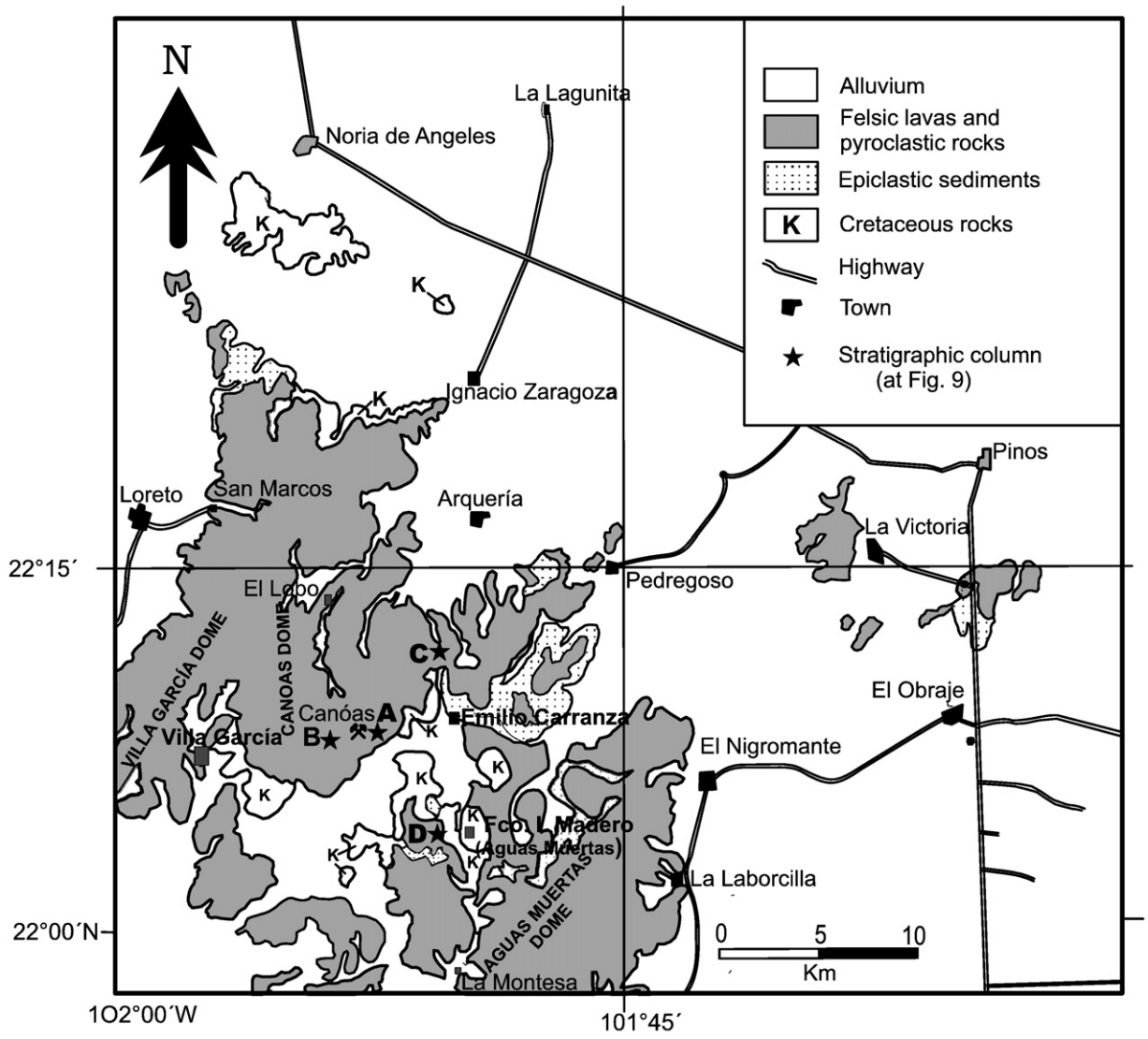

Fig. 8. Generalized geologic map of the Aguas Muertas dome complex. The letters in the map refer to the stratigraphic columns of Fig. 9. A) Canoas dome, B) El Cuije dome, C) Emilio Carranza dome and D) Aguas Muertas dome.

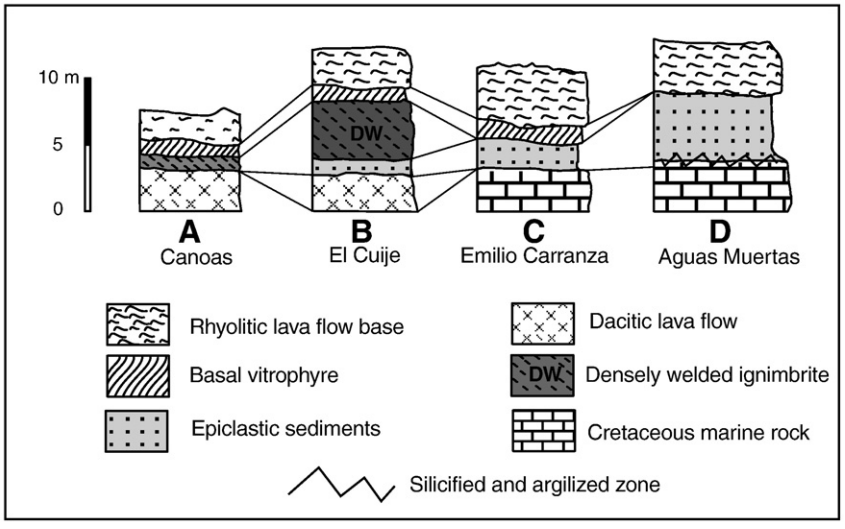

Fig. 9. Measured stratigraphic sections of the Aguas Muertas dome complex. Labels of the columns correspond to sections indicated in the map shown in Fig. 8.

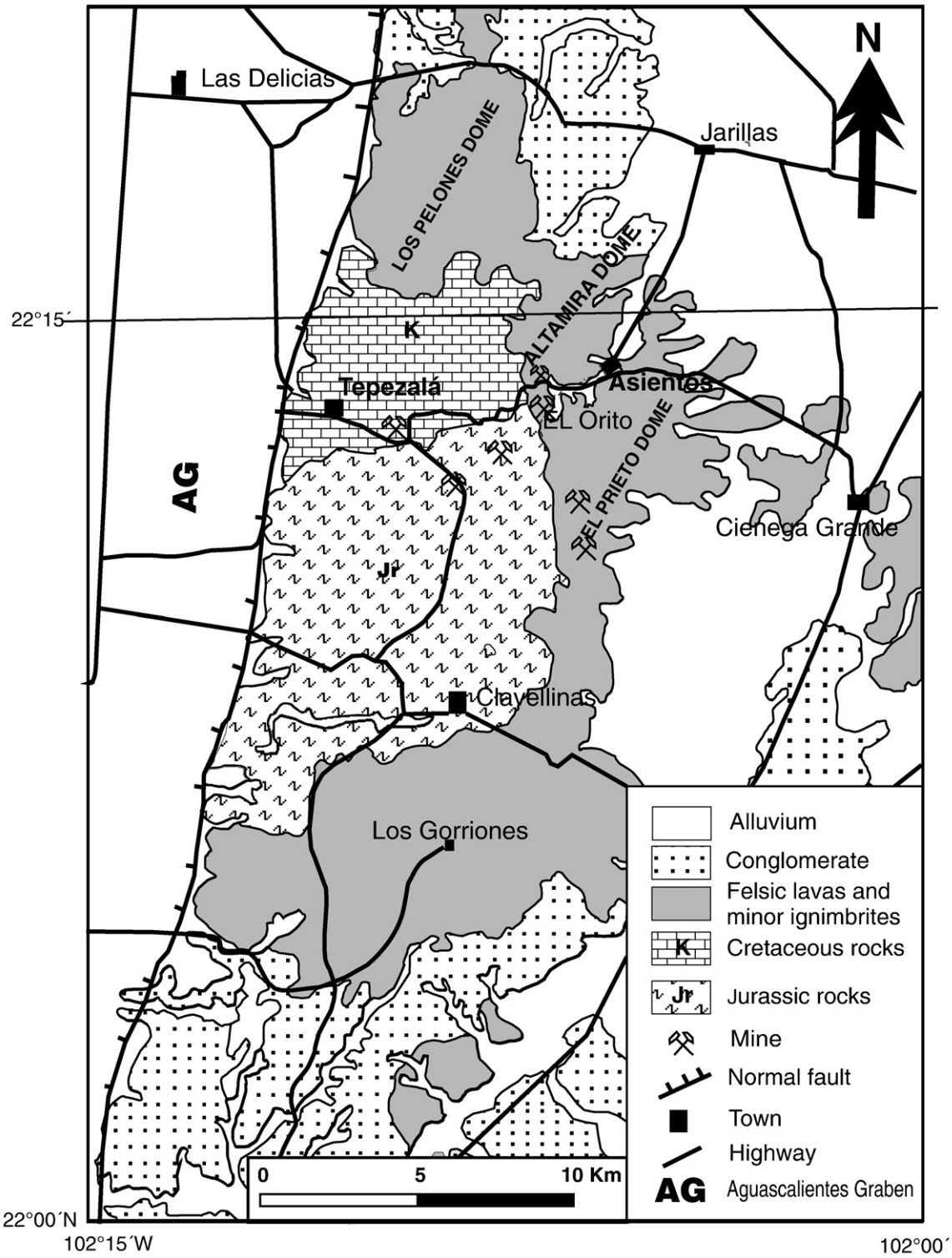

Fig. 10. Generalized geologic map of the Asientos–Tepezalá area, which is part of the Aguas Muertas dome complex.

containing 10 vol.% of quartz and sanidine phenocrysts, 2–3 mm, in a devitrified matrix with flow banding.

El Gallo dome is located near the city of Aguascalientes, in the northern part of the complex (Fig. 12). The sequence is formed at the base by marine Mesozoic sedimentary rocks, and widespread Oligocene ignimbrites with eutaxitic fabric. Covering them are three rhyolitic lavas with a very similar appearance, which form El Gallo dome. They are brown gray, with quartz and sanidine phenocrysts, 1–3 mm, and a few ferromagnesian minerals altered to hematite, and devitrified and fluidal matrix. The ignimbrites appear to be distributed in a radial pattern outward from the El Gallo dome, suggesting that their vent coincided with that of El Gallo dome.

4. Geochronology

Seven new K–Ar ages were performed in this study from representative samples of lava domes (Table 1). The analyses were done in the laboratory of geochronology of the Université de Bretagne

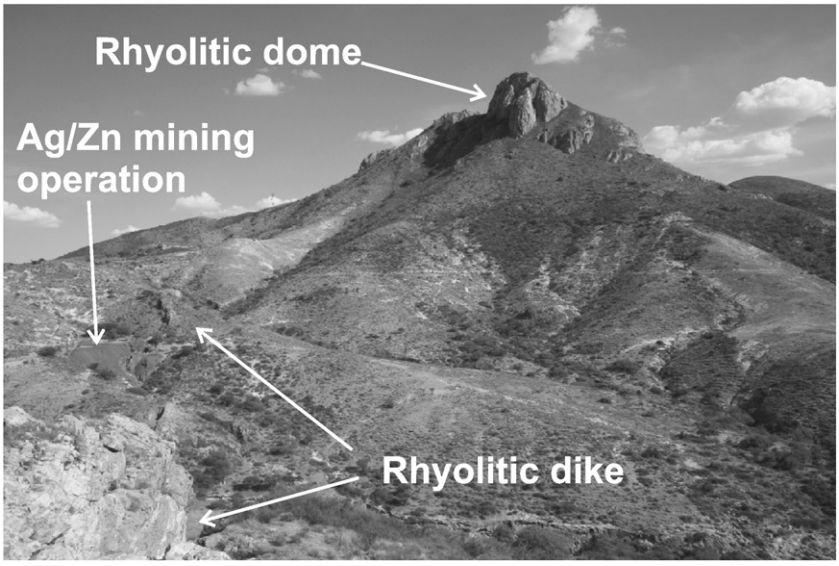

Fig. 11. View to the north of the Cerro Altamira rhyolitic dome. In the foreground is one of the NNE-trending rhyolitic dikes of the Asientos–Tepezalá–El Orito mining district within the Aguas Muertas dome complex. Dike's thickness ranges from 3 to 5 m. The dike cuts Mesozoic carbonated sedimentary rocks. Hydrothermal alteration and Ag/Pb/Zn mineralization are associated to these dikes and domes.

Occidentale, at Brest, France. Analyses were performed on separated minerals and whole rocks. Rock samples were fragmented to 300–150 μm; a portion was pulverized for analysis of K by atomic absorption technique. A detailed description of the methods can be found in Bellon et al. (1981). K–Ar ages were calculated using the decay constants of Steiger and Jäger (1977) and $\pm 1\sigma$ error estimates were calculated using the equation of Cox and Dalrymple (1967).

Results indicate that lava domes of Aguas Muertas complex were emplaced between 32.3 ± 0.5 and 29.5 ± 0.5 Ma (samples SLP-9, 10, 13 and 15; Table 1). Two samples from the lava domes of El Pájaro complex yielded 32.9 ± 0.6 and 28.5 ± 0.5 Ma (SLP-11 and 16, Table 1). A single age of 33.3 ± 0.5 Ma was obtained for the Santa Inés dome complex (sample SLP-12, Table 1). Fig. 14 shows a plot of these new ages *vs.* time compared with ages obtained from previous works on other volcanic rocks of the Mesa Central.

5. Geochemistry of the dome complexes

5.1. Method

Twenty two representative samples of the volcanic complexes were selected for chemical analyses, Aguas Muertas ($n=7$), El Pájaro ($n=3$), Ojuelos ($n=8$), and Santa Inés ($n=4$). The XRF technique was applied for the major and some trace elements (Rb, Sr, Ba, Y, Zr, Nb). The ICP-MS technique was used for the REE and Th. All analyses were performed at the Laboratorio Universitario de Geoquímica e Isotópos (LUGIS) of the Universidad Nacional Autónoma de México (UNAM). Details of the analytical methods can be found in Lozano and Bernal (2005) and by Morton et al. (1997). Results are reported in Table 2. The major elements data were re-calculated to sum 100%, volatiles-free, using the SINCLAS program (Verma et al., 2002) for CIPW Norm calculation and for plotting in diagrams.

5.2. Major and trace elements results

From the total alkalis-silica classification, (TAS diagram, after Le Bass et al., 1986; Fig. 15) it can be observed that all samples from the Aguas Muertas complex are rhyolites, varying from low K to high K rocks; the Pájaro complex includes rhyolites with moderate K content; the Ojuelos complex varies from low K rhyolite to trachydacite (normative *qz* between 22 and 43%; Table 2); the Santa Inés complex varies from trachydacite (*qz* normative ~25%; Table 2) to the rhyolite field. In the SiO_2 *vs.* K_2O diagram of Peccerillo and Taylor (1976) the samples classify in the calc-alkaline field with moderate to high K (Fig. 15).

The variations in major elements, considering all the complexes are (calculated volatiles-free) $SiO_2 = 66.3–79.7\%$; $Al_2O_3 = 11.8–16.3\%$; $TiO_2 = 0.07–0.53\%$; $Fe_2O_3 = 1.6–7.5\%$; $MgO = 0.08–0.67\%$; $CaO = 0.1–2.3\%$; $Na_2O = 0.7–4.2\%$; $K_2O = 4.2–8.1\%$ (Fig. 15). In general, the major elements show depletion with enrichment of SiO_2, except for Na_2O and K_2O that remain with little change (Fig. 15). The CIPW norm was calculated with the SINCLAS program (Verma et al., 2002). Observed variations are, $qz = 22–46\%$, $or = 25–47\%$; $ab = 6–35\%$; $an = 0–10\%$. The trace elements (Rb, Sr, Zr, Ba, Nb, Th) show different tendencies with respect to SiO_2; for instance, Ba, Sr and Zr become lower as SiO_2 increases, while Nb, Rb and Th increase with SiO_2 (Fig. 16). Ba has concentrations of up to 2500 ppm, whereas the rest of the elements do not exceed 1000 ppm (Fig. 16). Nb has values up to 80 ppm, but in general ranges between 20 and 60 ppm (Fig. 16). Th contains up 90 ppm, but this high value was observed only in one sample; in general, Th ranges from 10 to 50 ppm. Zr generally ranges between 100 and 400 ppm but in a single case it is near to 1000 ppm (Fig. 16).

5.3. Rare earth elements results

REE data are shown in the plot of REE *vs.* chrondite-normalized values (Fig. 17), normalizing to chondrite C1 after Sun and McDonough (1989). REE patterns show a slightly horizontal pattern with a low negative Eu anomaly. The light REE (LREE) are more fractionated than the heavy REE (HREE), and these last ones form a slightly concave up pattern due to the relative increase of Yb and Lu.

In the Aguas Muertas and Ojuelos complexes the LREE to HREE fractionation is slightly more marked. The HREE have in general a more horizontal pattern. In these two complexes the Eu negative anomaly is relatively more pronounced and the HREE are nearly horizontal, with a slight augmentation in Lu (Fig. 17, B and C).

The REE pattern of Santa Inés complex show a very similar tendency as the other volcanic complexes, with a light fractionation of LREE with respect to HREE, but in this case, the Eu-negative anomaly is relatively small (Fig. 17D).

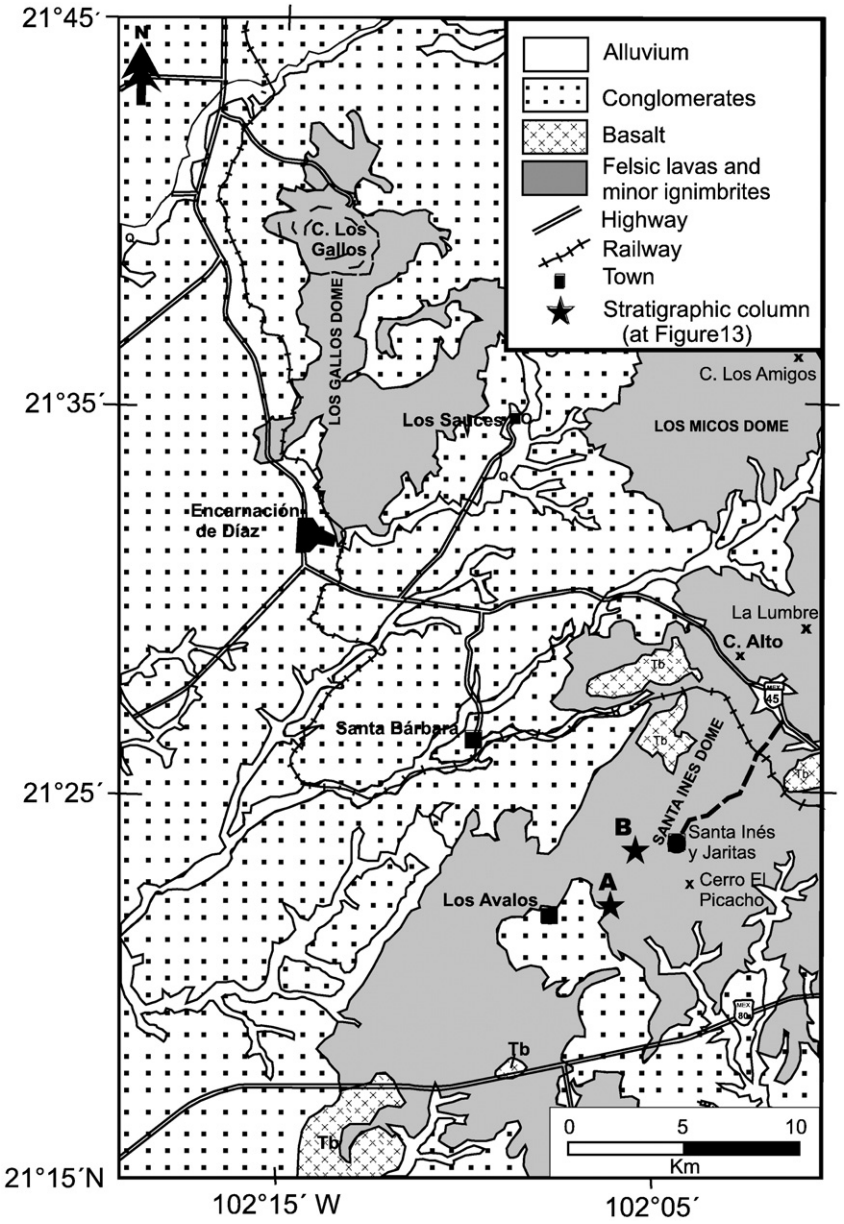

Fig. 12. Generalized geologic map of the Santa Inés dome complex.

Webster et al. (1996) indicate that the rhyolitic lava flows of El Pájaro complex are very similar, especially in the REE patterns, with the rhyolitic rocks of the Mexican Tin Rhyolite belt (Lee-Moreno, 1972; Huspeni et al., 1984).

6. Discussion

The formation of the SMO involved several tectono-magmatic events, from a long-lived arc-volcanism stage, mainly andesitic–dacitic, which ended in the Eocene–Oligocene (McDowell and Clabaugh, 1979; Damon et al., 1983; Aguirre-Díaz and McDowell, 1991), to an extension-related stage, mainly dacitic-rhyolitic, which coincided with the Basin and Range faulting during the Oligocene–Miocene (McDowell and Clabaugh, 1979; Damon et al., 1981; Aguirre-Díaz and McDowell, 1991; McDowell and Mauger, 1994; Aguirre-Díaz and Labarthe-Hernández, 2003; Aguirre-Díaz et al., 2008). Finally, there was a late stage of mafic volcanism in Early Miocene associated with extension (Cameron et al., 1980; Aguirre-Díaz and McDowell, 1993; Aranda-Gómez et al., 2000; Aguirre-Díaz et al., 2008). Oligocene–Miocene felsic magmatism is calc-alkaline and it has been interpreted as subduction-related (McDowell and Clabaugh, 1979; Damon et al., 1983; Aguirre-Díaz and McDowell, 1991; Ferrari et al., 2002; Ferrari et al., 2005). Aguirre-Díaz and McDowell (1991) refer to the voluminous rhyolitic Eocene–Oligocene volcanism as the Ignimbrite Flare-up, and believe it was mainly produced between the end of the subduction regime and the initiation of the extensional regime, when crustal relaxation may have been prevalent. The Early Miocene mafic magmatism has been associated with the transition from a continental-arc regime to intra-plate volcanism, as this phase includes both subalkaline andesites (the SCORBA suite of Cameron et al., 1980) and alkaline basalts, such as hawaiites (Aguirre-Díaz and McDowell, 1993). It is generally accepted that the formation of the mid-Tertiary felsic and voluminous volcanic rocks of the SMO coincided in time and space with the Basin and Range extension, which formed normal faults and grabens with a NW–SE to NE–SW general trend (Stewart, 1978; Labarthe-Hernández et al., 1982; Henry and Aranda-Gómez, 1992; Nieto-Samaniego et al., 1996; Stewart, 1998; Aguirre-Díaz and Labarthe-Hernández, 2003; Nieto-Samaniego

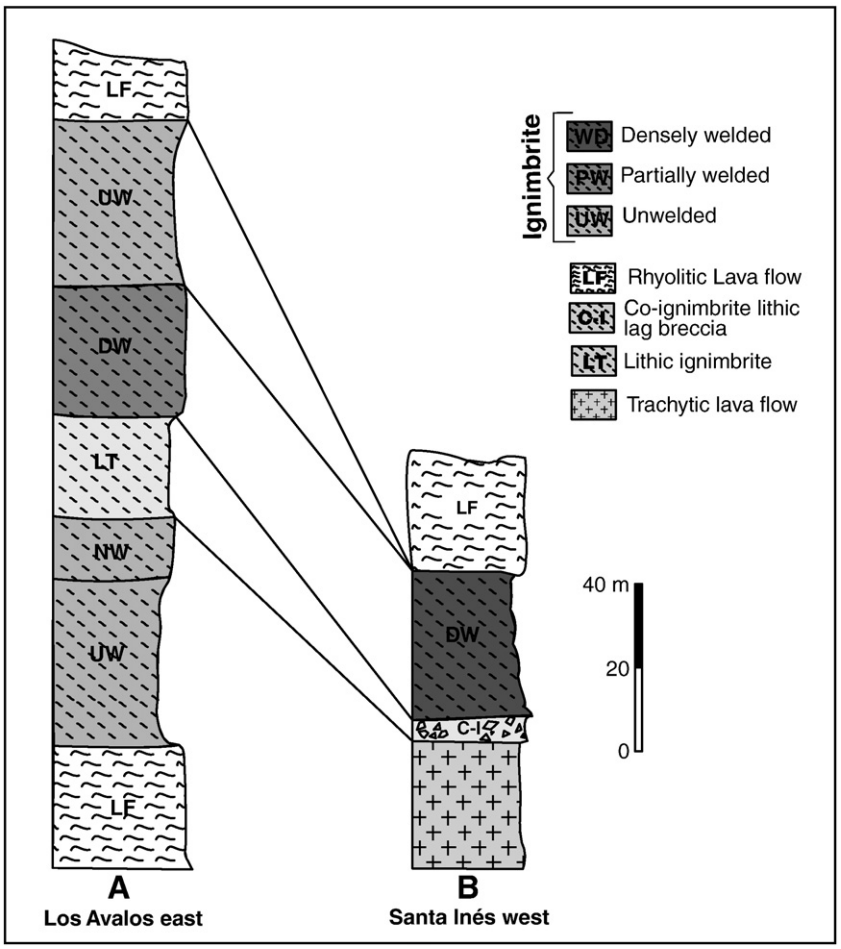

Fig. 13. Measured stratigraphic sections of two localities of the Santa Inés dome complex. The letters in the map refer to the stratigraphic columns of Fig. 12. A) Los Avalos east, B) Santa Inés west.

et al., 2005; Aguirre-Díaz et al., 2008; Tristán-González et al., 2009a,b). The overlapping of felsic magmatism and extension-produced fissural type eruptions throughout the SMO, either as explosive eruptions that formed ignimbrites, or effusive eruptions that formed domes

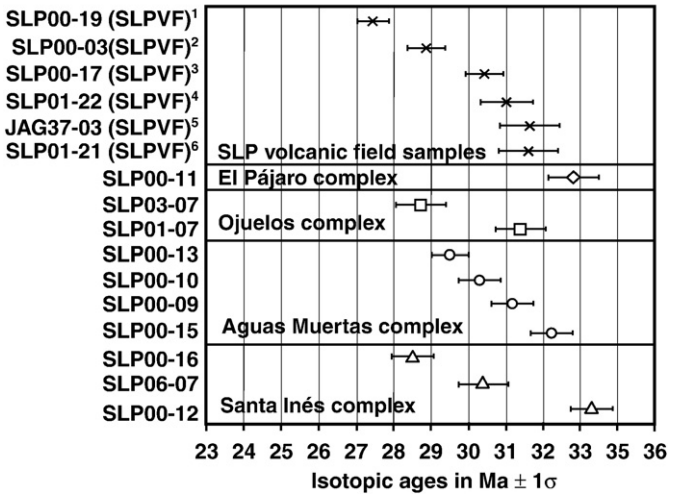

Fig. 14. Bar diagram showing the ages and corresponding analytical errors to 1σ std. dev. of dated units of the southern Mesa Central dome complexes. See Table 1 for details of age analyzes. Superscript numbers in each sample number correspond to references indicated in Table 1.

(Aguirre-Díaz and Labarthe-Hernández, 2003; Torres-Hernández et al., 2006; Tristán-González et al., 2006; Aguirre-Díaz et al., 2008).

In the southeastern portion of the SMO, and more specifically in the southern part of the Mesa Central, there was a large event of effusive felsic volcanism during the Oligocene, represented by several complexes of trachydacitic to rhyolitic domes. Due to the alignment of these domes with the main systems of normal Basin and Range faults, a structural control of the felsic magmas by these faults can be deduced. These dome complexes are groups of lava domes that were emplaced close to each other and aligned with the regional tectonic trending. On this basis, we interpret these complexes as fault-controlled emissions that formed chains of lava domes or dome clusters that occurred possible as passive magmatism. There are several complexes in the southern Mesa Central, from which we have studied 4 representative cases, I—El Pájaro, II—Ojuelos, III—Aguas Muertas, IV—Santa Inés. Regional geophysics and geologic studies indicate that this zone of the Mesa Central displays a relative thinning of the crust to a 30 to 33 km thickness compared to the about 40–42 km thickness of the crust to the west, or the 37 km thickness to the east (Meyer et al., 1958; Fix, 1975; Smith and Jones, 1979; Rivera and Ponce, 1986; Nieto-Samaniego et al., 1999). This thinning was apparently due to extension of the Basin and Range during the Oligocene–Miocene and we think that this favored the emplacement of the felsic domes between 33 and 28 Ma, which corresponds to the domes age range. Similar conditions are mentioned by Smith and Jones (1979), who propose an incipient rifting with NNW orientation in an extensional regime and the consequent thinning of the crust that can permit the extrusion of felsic magmas across a brittle crust.

Table 2
Major and trace elements of volcanic units from the volcanic complexes of SE portion of the Sierra Madre Occidental.

Sample	MT2-1	MT2-3	D3	SLP 10-07	MT2-2	MT2-4	MT2-5	MT2-6	MT2-10	MT2-12	SLP02-07	MT2-13	SLP01-07	MT2-16
Rock type	R	R	R	R	R	R	R	R	R	TD	TD	R	R	R
Complejo Volcánico	El Pájaro	El Pájaro	El Pájaro	El Pájaro	Ojuelos	Ojuelos	Ojuelos	Ojuelos	Ojuelos	Ojuelos	Ojuelos	Ojuelos	Ojuelos	Ojuelos
SiO_2	73.601	72.023	75.809	77.00	73.843	71.01	73.92	68.83	75.18	64.08	66.20	74.97	74.70	73.68
TiO_2	0.144	0.096	0.103	0.10	0.079	0.29	0.20	0.22	0.13	0.50	0.51	0.20	0.17	0.09
Al_2O_3	13.603	14.039	12.799	11.38	13.359	12.95	12.85	15.55	12.08	14.23	13.80	11.98	12.50	12.72
Fe_2O_3	2.924	2.837	1.932	1.70	1.697	4.36	3.41	3.92	2.36	7.61	7.15	3.11	2.17	3.71
MnO	0.041	0.035	0.013	0.01	0.03	0.06	0.06	0.03	0.03	0.23	0.06	0.02	0.02	0.02
MgO	0.168	0.238	0.179	0.08	0.174	0.24	0.28	0.24	0.22	0.43	0.16	0.21	0.13	0.41
CaO	0.573	0.702	0.238	0.34	0.699	1.23	0.61	0.61	0.49	1.29	0.96	0.54	0.43	0.66
Na_2O	3.359	3.015	2.111	2.03	1.83	3.01	2.69	2.42	2.96	2.98	2.97	2.52	2.50	2.73
K_2O	5.304	5.548	4.589	4.01	5.044	5.01	4.78	5.09	5.36	5.52	5.50	5.36	5.20	4.86
P_2O_5	0.017	0.017	0.017	0.02	0.012	0.05	0.02	0.04	0.02	0.14	0.10	0.03	0.03	0.05
LOI	0.8	1.4	1.73	2.49	3.83	1.10	1.50	3.07	0.76	2.31	1.90	1.24	1.61	1.61
Total	100.53	99.95	99.52	99.16	100.6	99.32	100.32	100.05	99.61	99.35	99.31	100.21	99.46	100.56
SiO_2 (adj)	73.896	73.181	77.598	79.723	76.376	72.45	74.92	71.125	76.133	66.295	68.207	75.866	76.422	74.598
Na_2O (adj)	3.372	3.063	2.161	2.102	1.893	3.067	2.726	2.500	3.000	3.088	3.06	2.555	2.558	2.763
K_2O (adj)	5.325	5.637	4.697	4.152	5.217	5.109	4.843	5.267	5.434	5.715	5.667	5.429	5.32	4.924
qz	32.133	31.564	46.022	50.526	43.33	31.563	38.373	34.184	36.274	22.032	25.668	38.478	39.893	37.185
or	31.469	33.312	27.758	24.537	30.83	30.192	28.62	31.126	32.113	33.774	33.490	32.083	31.439	29.099
ab	28.533	25.918	18.286	17.786	16.018	25.952	23.066	21.154	25.385	26.13	25.893	21.62	21.645	23.38
an	2.742	3.426	1.099	1.609	3.508	5.897	2.884	2.878	2.342	5.707	4.234	2.536	1.980	3.028
c	1.342	1.869	4.059	3.24	3.77	0.478	2.238	5.204	0.562	1.367	1.498	1.122	2.095	1.903
hy	1.153	1.451	1.077	0.781	1.074	1.882	1.770	1.999	1.139	3.962	2.555	1.271	0.849	2.284
ap	0.039	0.039	0.039	0.049	0.028	0.127	0.056	0.102	0.044	0.334	0.239	0.065	0.072	0.106
Ba	214	43	80	42	17	–	122	532	44	2665	2425	170	138	59
Nb	28	35	38	30	21	–	49	28	50	18	27.5	48	32.5	26
Th	29	29	88	19.7	31	–	39	24	44	12	13	29	20	30
Sr	14	11	9	27	6	–	15	40	1	155	130	16	22	12
Rb	180	287	232	207	313	–	170	160	316	148	168	204	209	241
Zr	368	189	241	165	132	–	405	509	352	618	955	437	47	183
La	38.07	19.24	13.33	30.5	19.08	52.90	50.18	51.03	16.58	–	230	–	81.5	–
Ce	33.49	59.88	31.55	43	31.60	35.81	12.01	11.68	81.79	–	167	–	123	–
Pr	11.56	5.36	3.18	–	6.05	15.7	15.28	16.76	3.76	–	–	–	–	–
Nd	47.09	20.20	11.90	16.3	24.50	63.1	57.45	66.29	13.99	–	200	–	72	–
Sm	13.03	5.12	3.06	3.4	6.65	13.61	9.71	14.48	4.86	–	34.5	–	12.3	–
Eu	1.32	0.22	0.36	0.34	0.17	2.08	0.63	1.29	0.15	–	4.6	–	0.83	–
Gd	16.78	5.69	3.34	3.7	6.76	14.06	8.4	14.43	7.7	–	32	–	8.8	–
Tb	3.09	1.18	0.81	–	1.28	2.34	1.24	2.49	2.03	–	–	–	–	–
Dy	18.33	7.23	5.47	3.55	7.19	13.24	6.42	14.08	14.08	–	23	–	6.75	–
Ho	4.26	1.71	1.39	–	1.60	2.9	1.3	3.03	3.48	–	–	–	–	–
Er	10.88	4.60	3.98	2.5	4.09	7.27	1.3	3.03	9.3	–	11	–	3.4	–
Tm	1.72	0.80	0.73	–	0.69	1.12	0.55	1.19	1.52	–	–	–	–	–
Yb	10.07	4.70	4.30	2.73	3.80	6.3	3.09	6.68	8.63	–	9.18	–	3.09	–
Lu	1.74	0.84	0.75	–	0.68	1.08	0.55	1.13	1.42	–	–	–	–	–

(continued on next page)

Table 2 (*continued*)

Muestra	D4	D2	D6	D7	D8	MT2-7	MT2-14	D5	SLP06-07	SLP07-07	SLP08-07	MT2-8	MT2-9	MT2-15	SLP05-07
Tipo de roca	R	R	R	R	R	R	R	TD	R	R	R	R	R	R	R
Complejo Volcánico	Aguas Muertas	Aguas Muertas	Aguas Muertas	Aguas Muertas	Aguas Muertas	Aguas Muertas	Aguas Muertas	Santa Inés	Santa Inés	Santa Inés	Santa Inés	Santa Inés	Santa Inés	Santa Inés	Santa Inés
SiO_2	65.872	74.966	74.894	73.715	73.833	76.29	68.56	67.722	70.50	72.40	71.50	68.66	74.01	74.65	76.30
TiO_2	0.439	0.144	0.102	0.074	0.208	0.08	0.24	0.275	0.33	0.23	0.20	0.25	0.08	0.07	0.14
Al_2O_3	13.951	12.408	12.761	14.061	12.718	12.04	15.35	16.012	13.12	13.3	12.95	13.91	13.82	13.08	12.15
Fe_2O_3	4.845	2.268	1.764	1.809	3.198	1.93	3.78	3.732	4.70	2.83	2.46	5.29	2.10	1.96	1.84
MnO	0.021	0.017	0.011	0.036	0.041	0.05	0.04	0.04	0.03	0.03	0.02	0.05	0.02	0.03	0.01
MgO	0.248	0.177	0.117	0.331	0.32	0.23	0.19	0.379	0.11	0.15	0.64	0.33	0.16	0.25	0.08
CaO	0.232	0.304	0.118	0.75	0.319	0.77	0.56	2.241	0.70	1.10	0.79	0.83	0.10	0.69	0.41
Na_2O	1.02	2.411	0.735	2.554	2.242	2.74	3.02	3.604	2.92	3.00	2.17	3.12	4.23	2.89	2.92
K_2O	4.896	5.201	7.954	4.949	5.425	4.72	7.02	4.464	5.37	4.85	4.90	5.44	4.99	4.16	5.20
P_2O_5	0.196	0.027	0.046	0.022	0.03	0.02	0.08	0.127	0.04	0.06	0.05	0.06	0.03	0.02	0.02
LOI	7.98	1.57	1.01	1.39	1.41	0.84	1.54	0.95	1.33	1.44	3.62	1.32	0.85	1.98	0.69
Total	99.7	99.49	99.58	99.69	99.74	99.74	100.41	99.54	99.15	99.39	99.30	99.27	100.40	99.81	99.76
SiO_2 (adj)	72.028	76.64	76.094	75.056	75.201	77.206	69.46	68.815	72.237	77.082	74.825	70.279	74.416	76.388	77.082
Na_2O (adj)	1.115	2.465	0.747	2.600	2.284	2.777	3.061	3.662	2.992	5.253	2.271	3.2	4.249	2.964	2.95
K_2O (adj)	5.354	5.317	8.081	5.039	5.526	4.786	7.116	4.536	5.502	8.025	5.128	5.569	5.020	4.255	5.253
qz	43.697	40.824	40.352	38.287	39.263	40.473	22.808	24.551	31.63	34.412	39.019	27.441	29.897	40.684	38.706
or	31.64	31.421	47.756	29.779	32.656	28.283	42.053	26.806	32.515	29.3	30.304	32.911	29.666	25.145	31.043
ab	9.435	20.858	6.321	22.000	19.326	23.498	25.901	30.987	25.317	25.952	19.216	27.077	35.954	25.08	24.962
an	–	1.36	0.288	3.646	1.416	3.76	2.261	10.454	3.289	5.178	3.763	3.839	0.31	3.403	1.923
c	7.625	2.376	2.884	3.249	2.696	1.061	1.994	1.504	1.36	1.287	2.886	1.536	1.356	2.657	1.03
hy	2.762	1.048	0.664	1.46	1.703	1.216	1.243	2.088	1.503	1.098	2.429	2.486	0.874	1.356	0.557
ap	0.447	0.065	0.109	0.051	0.07	0.044	0.199	0.299	0.095	0.141	0.12	0.125	0.07	0.044	0.046
Ba	697	42	112	36	99	85	361	1026	1350	820	920	832	500	540	1220
Nb	13	54	24	25	44	21	38	15	26.5	17	16	25	77	28	30.5
Th	22	39	18	28	44	30	29	15	15.7	14.8	15.9	22	64	29	21.2
Sr	199	5	25	17	7	11	25	184	88	101	125	64	0.5	11	17
Rb	168	329	404	297	217	243	217	150	192	175	193	184	370	240	230
Zr	229	306	134	134	401	158	429	302	80	118	64	435	380	161	32
La	24.82	44.59	–	–	–	27.87	–	–	86	90	87	51.34	–	–	70
Ce	19.26	49.87	–	–	–	47.08	–	–	216	159	146	63.98	–	–	107
Pr	7.38	14.26	–	–	–	8.13	–	–	–	–	–	15.06	–	–	–
Nd	29.45	56.15	–	–	–	32.04	–	–	115	78	81	60.45	–	–	67
Sm	6.39	13.32	–	–	–	7.34	–	–	24.4	15	15	13.38	–	–	12.5
Eu	0.63	0.21	–	–	–	0.25	–	–	2.66	1.44	1.16	1.8	–	–	0.67
Gd	5.89	13.99	–	–	–	6.57	–	–	19.3	14.8	13.2	13.42	–	–	9.9
Tb	0.90	2.58	–	–	–	1.13	–	–	–	–	–	2.27	–	–	–
Dy	4.34	15.09	–	–	–	6.23	–	–	15.3	12.9	10.15	12.62	–	–	8.1
Ho	0.86	3.45	–	–	–	1.37	–	–	–	–	–	2.77	–	–	–
Er	2.08	8.88	–	–	–	3.57	–	–	7.2	7	5.4	6.9	–	–	4.7
Tm	0.36	1.43	–	–	–	0.63	–	–	–	–	–	1.09	–	–	–
Yb	1.83	8.32	–	–	–	3.67	–	–	6.38	6.03	4.7	6.08	–	–	4.46
Lu	0.36	1.42	–	–	–	0.67	–	–	–	–	–	1.06	–	–	–

R — rhyolite; TD — trachydacite. Classification TAS (Le Bass et al., 1986). CIPW Norm using adjusted to 100% anhydrous values, the Fe_2O_3/FeO relation of Middlemost (1989) by means of program SINCLAS (Verma et al., 2002). Analyses were performed by XRF for major elements and ICP-MS for trace elements.

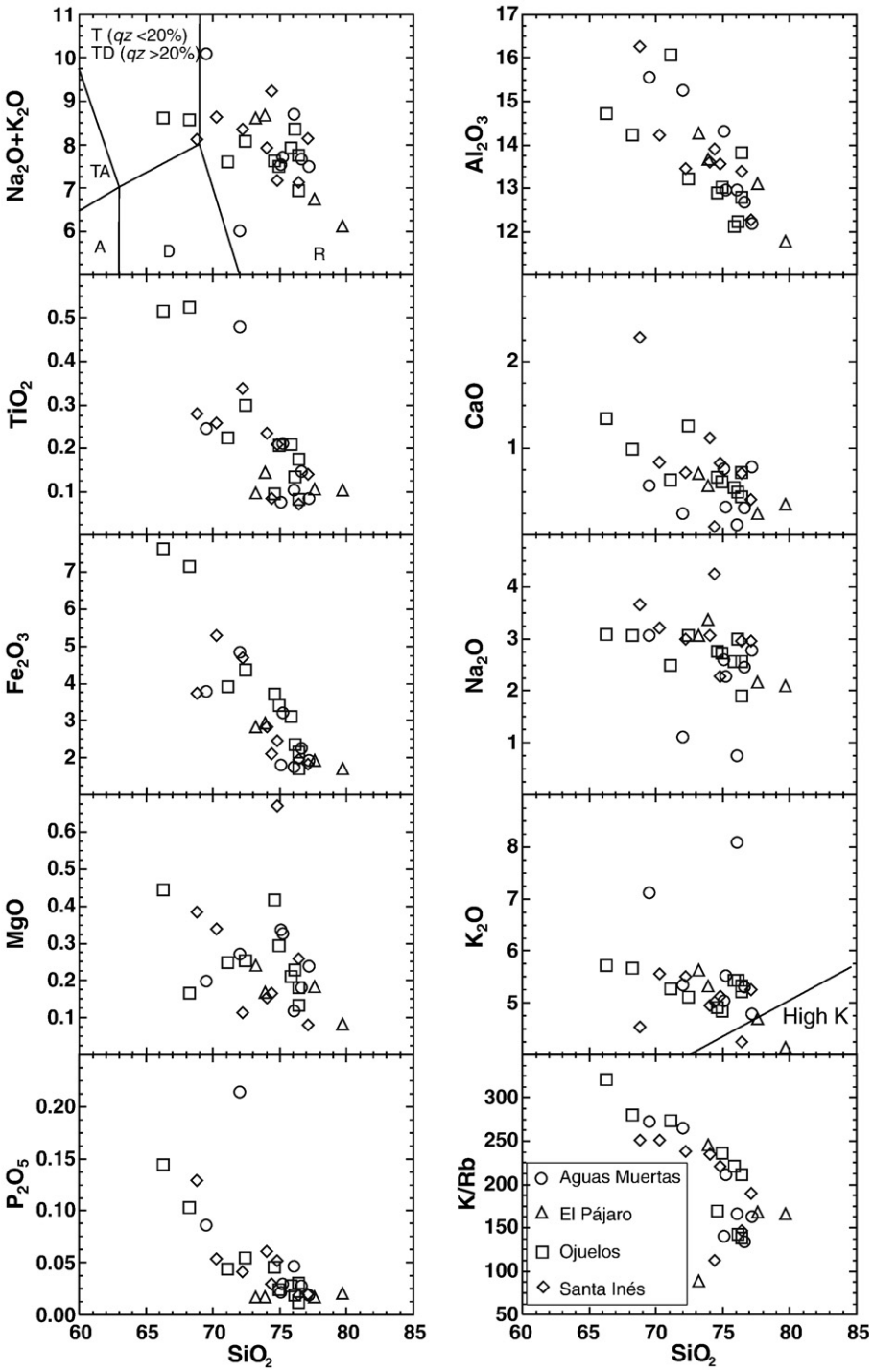

Fig. 15. Major elements geochemistry plots. Harker diagrams including Total Alkalis-Silica, TAS (Le Bass et al., 1986) and K_2O-Silica (Peccerillo and Taylor, 1976) classifications. TAS diagram labels: A — andesite, TA — trachyandesite, D — dacite, TD — trachydacite, T — trachyte, R — rhyolite. The use of normative quartz content in vol.% (*qz*) is used to distinguish trachydacite TD from trachyte T, following Le Bass et al. (1986).

Geochemical studies of the domes in the Mesa Central were mostly restricted to descriptive chemical classification purposes, with no inferences on the petrogenesis of these rocks (Labarthe-Hernández et al., 1982). Studies with petrogenetic aims are rare (e.g., Verma, 1984; Rodríguez-Ríos, 1997; Orozco-Esquivel et al., 2002; Rodríguez-Ríos et al., 2007). Verma (1984) reports Nd–Sr isotope results of felsic domes in Zacatecas, concluding that these magmas were generated by melting of continental crust. Rodríguez-Ríos (1997) reports a set of chemical analyses of major and trace elements in rhyolites and trachydacites with the same ages as those described here, but outside the study area. Orozco-Esquivel et al. (2002) made a geochemical and petrogenetic study in felsic and mafic lavas from localities at the southern Mesa Central, outside but near the study area. Orozco-Esquivel et al. (2002) elaborate a generalized model of magmatic evolution and conclude that the rocks were derived from partial melting from the continental crust, but due to a poor stratigraphic control in their study, it is not clear which volcanic episode corresponds with which magmatic process. Rodríguez-Ríos et al.

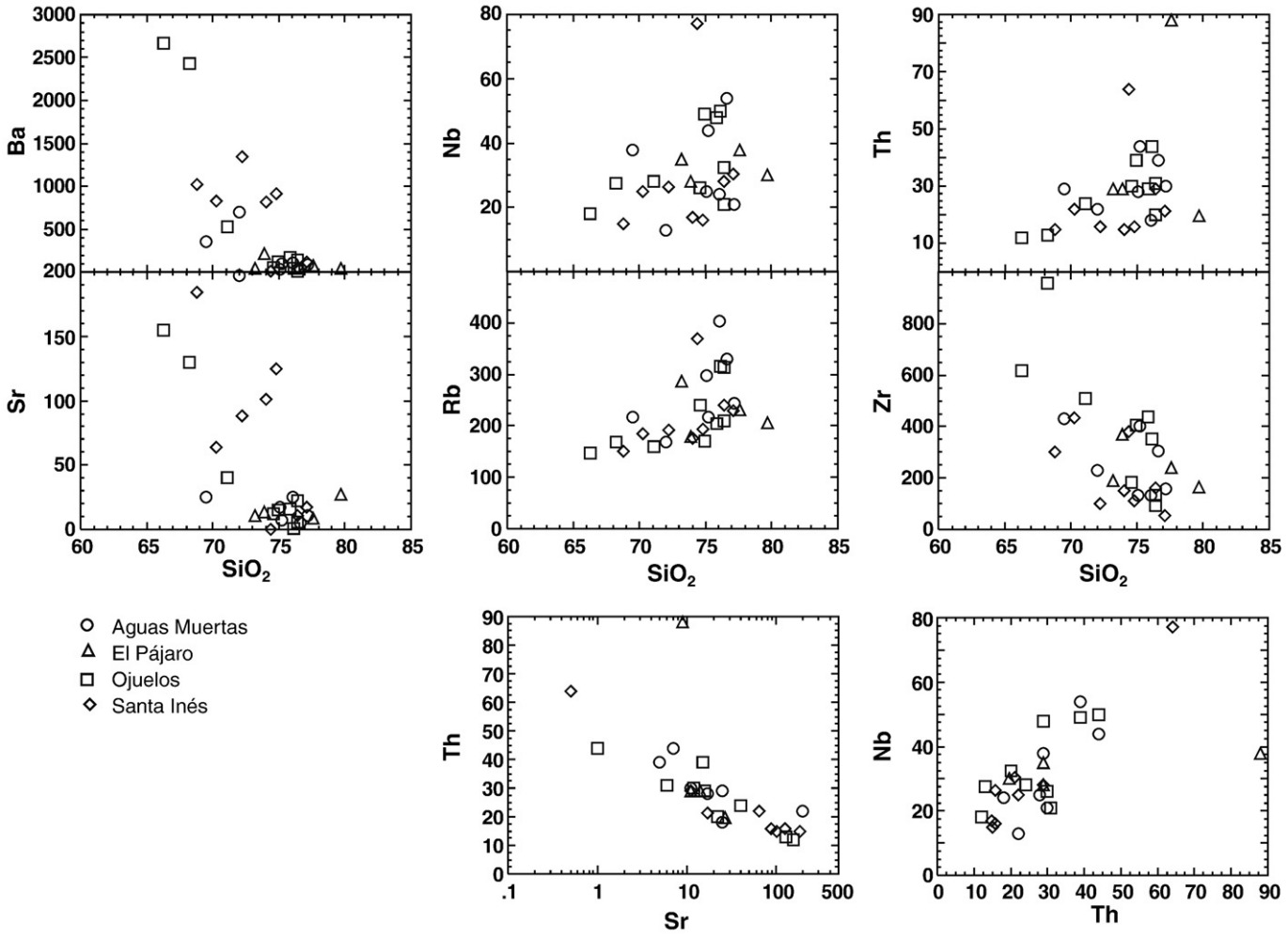

Fig. 16. Trace elements geochemistry plots. Variation diagrams with SiO_2 in wt.% and vertical axes in ppm.

(2007) conclude that these domes were originated by a combination of fractionated crystallization from a less evolved magma and contamination of Precambrian crust, without specifying if the magmas were derived by subduction or by intra-plate magmatism.

On the basis of the stratigraphical–geochronological control of the present work and the obtained chemical results, it can be deduced that 1) the felsic magmas of the southern portion of the Mesa Central were generated as magma batches from partial melting of the lower crust that initially produced trachydacitic magmas and a time later rhyolitic magmas (Fig. 15, Table 2), and 2) these magmas formed a rock suite (*sensu lato* Barker, 1983) that differentiated continuously between 33 and 28 Ma, probably in a similar way to the differentiation process described by Ngounouno et al. (2000) for the felsic volcanism of Cameroon. Textures and chemical data patterns indicate that although magmas experienced some crystal fractionation during their ascent, this process did not modify substantially the original trachydacytic and rhyolitic magma batches, and at most caused an evolving line from trachydacite/rhyolite to high-silica rhyolite.

According to the trace elements contents (Fig. 16), the magmas that produced the mid-Oligocene domes of the southern Mesa Central were generated in an intra-plate setting. We base this conclusion mainly upon the observed tendencies of key elements like Nb and Th, which remain constant or slightly enriched with differentiation (Fig. 16). If these magmas would have been generated by subduction, these elements would be depleted through differentiation (Gill, 1981), and this is not observed in the Nb–Th patterns. On the contrary, REE (Fig. 17) form flat or slightly negative patterns, and some data show concave positive forms, suggesting an intra-plate signature. It is known that the magmas generated by subduction form patterns with strong negative tendencies (Wilson, 1989), which is not the case in the Mesa Central domes of this study.

The observed variations of trace elements in multi-element plots (Fig. 17) suggest that the rocks were derived by a combined process involving partial melting of the crust, possibly metasomatized, and fractional crystallization, confirming the conclusions from other authors for similar rocks near this region (Verma, 1984; Orozco-Esquivel et al., 2002; Rodríguez-Ríos et al., 2007). In general, there is a depletion of Ba, Sr, and Zr with increasing SiO_2 (Fig. 16), whereas Nb, Rb and Th become enriched. Depletion of Ba, Sr and Zr can be related to partial melting of the crust. The enrichment in Nb, Rb, Th can be explained by an enriched original source, a non-depleted lithosphere, possible by metasomatism of the crustal base (Schaaf et al., 1994), and thus an intra-plate lithospheric setting, which remained enriched by slight processes of fractionated crystallization during the diapiric ascent. In summary, the data agree with a petrogenetic process involving partial melting of the lower crust involving or caused by fluids enriched in HFSE and LILE that show an affinity with an intra-plate fertile lithosphere.

The tectono-magmatic model for the emplacement of the mid-Oligocene felsic rocks of the southern portion of Mesa Central proposed here includes at least three continuous phases, each one related to an intense extensional pulse of the Basin and Range (Fig. 3). The first phase, at 33–32 Ma, is characterized by predominantly trachydacitic magmatism; the second one, at 32–31 Ma, is characterized by a mechanical

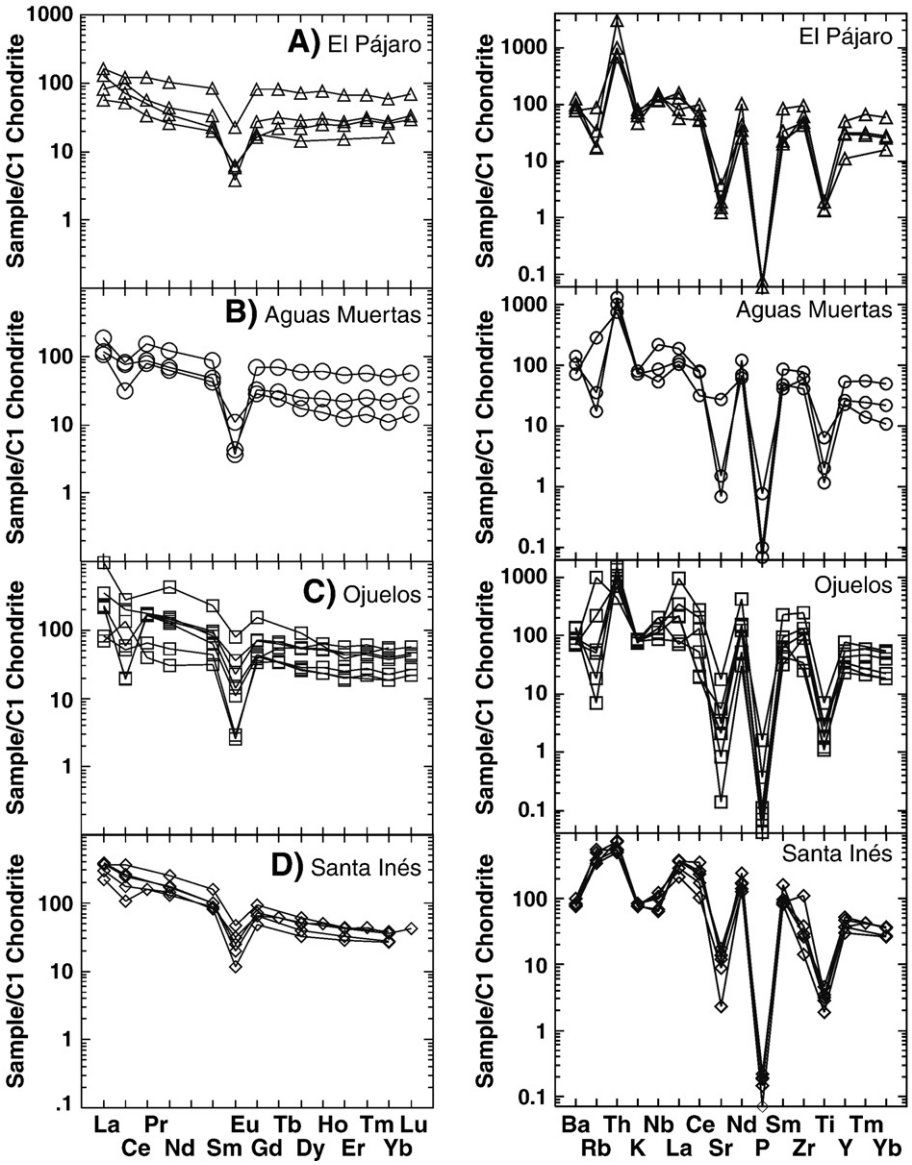

Fig. 17. Chondrite-normalized, Rare Earth and multi-elements plots using normalizing values of Sun and McDonough (1989) and element order suggested by Rock (1987).

mingling of trachydacitic and rhyolitic magmas (Fig. 18), where each magma conserved its original chemical characteristics (as defined by Bardintzeff and Daniel, 1992 and Aguirre-Díaz, 2001); and the third phase, at 31–28 Ma, is characterized by rhyolitic magmas of high silica content (up to 76 wt.% SiO_2). According to some authors, the rhyolitic rocks of the Mesa Central are derived from contamination of granitic crust in the magma chamber (Burt et al., 1982; Webster et al., 1996; Orozco-Esquivel et al., 2002). Nevertheless, in our model we do not consider the existence of magma chambers for the trachydacitic and rhyolitic magmas. Instead, we propose a direct ascend of magmas from their generation zone at the base of the crust to the surface (Fig. 18). Therefore, this crustal contamination, if was the case, would occur during the diapiric ascend of the magmas, or rather, the contamination signature could have been inherited from the original source, by the partial melting at the base of the crust. Hildreth (1981) proposed a similar mechanism in which magmas produced by partial melting in the lower crust ascend by diapirism during of episodic extensional events. There is a clear structural control of magmas by the regional Basin and Range faults, as most lava domes occur aligned with the general faulting trends. However, in younger units of this region and at other localities in the SMO, magmas formed large (batholith size) magma chambers at shallow levels that have been associated with graben type calderas or fissural type, voluminous, explosive, ignimbrite-forming eruptions (Aguirre-Díaz and Labarthe-Hernández, 2003; Aguirre-Díaz et al., 2008). The Oligocene effusive felsic volcanism occurred in response of the direct ascend of felsic magmas from its source to the surface, without stopping in crustal magma chambers. At the magma chambers, volatiles could be exsolved if pressure and composition allow, and thus produce explosive eruptions in the form of graben calderas, as occurred in many areas of the Sierra Madre Occidental (Aguirre-Díaz and Labarthe-Hernández, 2003; Aguirre-Díaz et al., 2008). There must be several factors involved in the formation or not of large-volume felsic magma chambers (batholiths), but a principal one must the crustal thickness. We propose that the relatively thin crust of southern Mesa Central and an intense extensional regime may have allowed ascend of felsic magmas across a brittle crust, perhaps in a passive way, without stopping in a magma chamber. The model

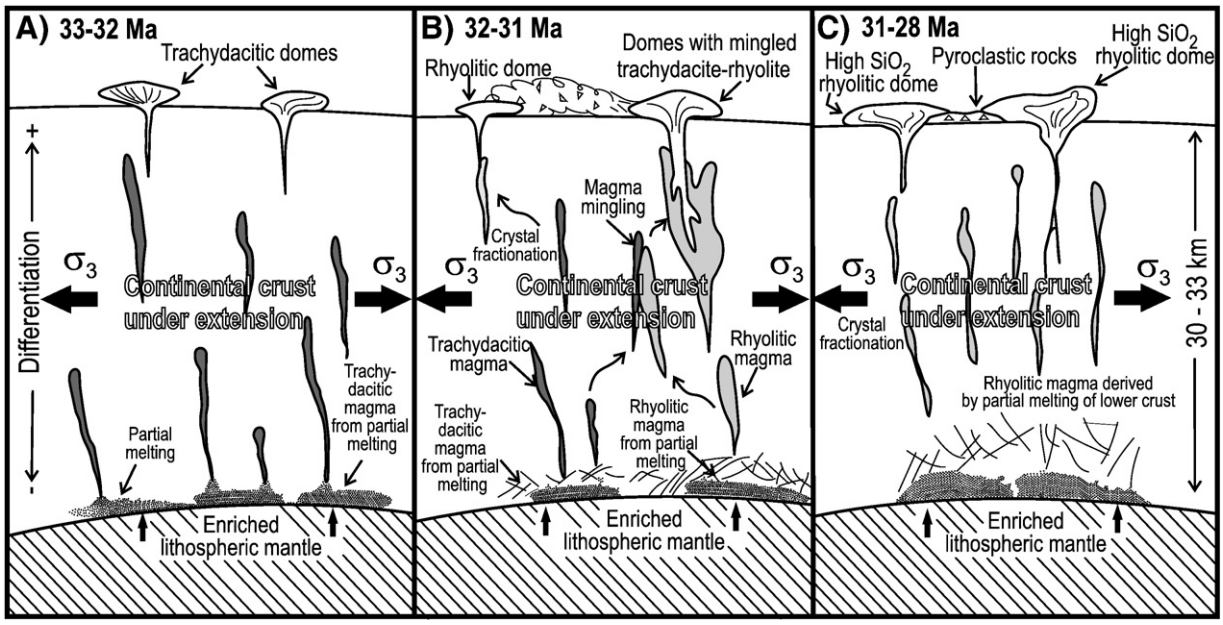

Fig. 18. Schematic model showing the tectono-magmatic episodes that are proposed in this work for the origin and emplacement of the mid-Oligocene felsic dome complexes of the southern Mesa Central. Three main episodes are proposed on the basis of the geology, geochronology and geochemistry data. The first one at 33–32 Ma caused the emplacement of trachydacitic domes, a second one at 32–31 Ma caused the emplacement of mingled trachydacitic and high-slilica rhyolitic domes, and the third one at 31–28 Ma caused high-silica rhyolitic domes. See text for further explanation.

proposed in this work would explain why in the southern Mesa Central effusive felsic volcanism (domes) was relatively much more abundant than the explosive felsic volcanism (ignimbrites), in a proportion of 4 to 1 (80 vol.% *vs.* 20 vol.%), as was mentioned in the Introduction.

7. Conclusions

The mid-Oligocene trachydacite-rhyolitic dome complexes in the southern portion of the Mesa Central, at the southeastern end of the volcanic province of the Sierra Madre Occidental, were extruded within the Basin and Range extensional regime.

The age range of these domes is 33–28 Ma. The first group of domes, 33–32 Ma and trachydacitic in composition, were extruded through normal faults and fissures and have NNE and NE–SW alignments. The second group, 32–31 Ma and with mingled compositions between trachydacite and rhyolite, were also controlled by extension and form NNE, NE–SW and NW–SE alignments. The third group, 31–28 Ma and rhyolitic in composition, were both controlled and then affected by NW–SE faulting.

The geochemical results indicate an origin by partial melting of the base of the continental crust, involving fluids enriched in HFSE and LILE that show an affinity with an intra-plate setting, and fractional crystallization that occurred possibly during magma ascent.

Considering that the crust in this region is relatively thin (30–33 km), we propose a tectono-magmatic model that includes three continuous phases of felsic magmas that ascended during extensional peaks, each pulse corresponding to each of the dome sets at 33–31, 32–31 Ma, and 31–28 Ma. In each set, magmas were generated at the base or in the lower crust and ascended directly to the surface without stopping to form magma chambers, favored by the intense extensional regime.

Acknowledgements

We thank Guillermo Labarthe-Hernández for providing valuable comments and help during preparation of this work. We thank the reviewers Laurent Michon and Joan Martí for their comments and suggestions that allowed an improved final version of the manuscript. We are grateful to the Instituto de Geología of Universidad Autónoma de San Luis Potosí for the logistical and financial support in order to carry out field work and chemical and radiometric dating analyses. Erasmo Mata-Martínez of the Instituto de Geología at the Universidad Autónoma de San Luis Potosí prepared the thin sections used in this work. This study was financed in part by grants to GJAD from CONACYT P46005-F and PAPIIT-UNAM IN-115302 and IN-114606.

References

Aguillón-Robles, A., Aranda-Gómez, J.J., Solorio-Munguía, J.G., 1994. Geología y tectónica de un conjunto de domos riolíticos del Oligoceno medio en el sur del estado de San Luis Potosí, México. Rev. Mex. Cienc. Geol. 11, 29–42.

Aguirre-Díaz, G.J., 2001. Recurrent magma mingling in successive ignimbrites from Amealco caldera, central Mexico. Bull. Volcanol. 63, 238–251.

Aguirre-Díaz, G.J., McDowell, F.W., 1991. The volcanic section at Nazas, Durango, Mexico, and the possibility of widespread Eocene volcanism within the Sierra Madre Occidental. J. Geophys. Res. 96, 13,373–13,388.

Aguirre-Díaz, G.J., McDowell, F.W., 1993. Nature and timing of faulting and synextensional magmatism in the southern Basin and Range, central-eastern Durango, Mexico. Geol. Soc. Am. Bull. 105, 1435–1444.

Aguirre-Díaz, G.J., Labarthe-Hernández, G., 2003. Fissure ignimbrites: fissure-source origin for voluminous ignimbrites of the Sierra Madre Occidental and its relationship with Basin and Range faulting. Geology 31, 773–776.

Aguirre-Díaz, G.J., Labarthe-Hernández, G., Tristán-González, M., Nieto-Obregón, J., Gutiérrez-Palomares, I., 2007. Graben-calderas. Volcano-tectonic explosive collapse structures of the Sierra Madre Occidental, México. European Geosciences Union Annual Meeting, Vienna 2007. Geophys. Res. Lett. 9, 04704.

Aguirre-Díaz, G.J., Labarthe-Hernández, G., Tristán-González, M., Nieto-Obregón, J., Gutiérrez-Palomares, I., 2008. Ignimbrite flare-up and graben-calderas of the Sierra Madre Occidental, Mexico. In: Martí, J., Gottsmann, J. (Eds.), Caldera Volcanism. Analysis, Modelling and Response. Developments in Volcanology, vol. 10. Elsevier, Amsterdam, pp. 143–180.

Aranda-Gómez, J.J., Labarthe-Hernández, G., Tristán-González, M., 1983. El volcanismo cenozoico en San Luis Potosí y su relación con la provincia volcánica de la Sierra Madre Occidental. Asociación de Ingenieros de Minas, Metalurgistas y Geólogos de México, Convención Nacional 15, Guadalajara, Jal., México, 261–287.

Aranda-Gómez, J.J., Aranda-Gómez, J.M., Nieto-Samaniego, A.F., 1989. Consideraciones acerca de la evolución tectónica durante el Cenozoico de la Sierra de Guanajuato y la parte meridional de la Mesa Central. Inst. Geol., Univ. Nac. Autón. Méx. 8 (1), 33–46. Revista.

Aranda-Gómez, J.J., Henry, C.D., Luhr, J.F., 2000. Evolución tectonomagmática post-paleocénica de la Sierra Madre Occidental y de la porción meridional de la provincia tectónica de Cuencas y Sierras, México. Bol. Soc. Geol. Mex. 53 (1), 59–71.

Bardintzeff, J.M., Daniel, C., 1992. Magmatic evolution of Pacaya and Cerro Chiquito volcanological complex, Guatemala. Bull. Volcanol. 54 (4), 267–283.
Barker, D.S., 1983. Igneous rocks. Prentice-Hall Inc. 417 pp.
Bellon, H., Quoc Buü, N., Chaumont, J., Philippet, J.C., 1981. Implantation ionique d'argon dans une cible support: applicationau traçage isotopique de l'argon contenu dans les minéraux et les roches. C.R. Acad. Sci. de Paris 292, 977–980.
Burt, D.M., Sheridan, M.F., 1987. Types of mineralization related to fluorine-rich silicic lava flow and domes. Geol. Soc. Am. 212, 103–109. Special Paper.
Burt, D.M., Bikun, J.V., Christiansen, E.H., Sheridan, M.F., 1982. Topaz rhyolites: distribution, origin, and significance for exploration. Ecol. Geol. 77, 1818–1836.
Cameron, K.L., Cameron, C., Babgy, W.C., Moll, E.J., Drake, R.E., 1980. Petrologic characteristics of mid-Tertiary volcanic suites, Chihuahua, Mexico. Geology 8, 87–91.
Campa, M.A., Coney, P.J., 1983. Tectono-stratigraphic terranes and mineral resource distribution in Mexico. Can. J. Earth Sci. 20, 1040–1051.
Carrillo-Bravo, J., 1971. La Plataforma Valles–San Luis Potosí. Bol. Asoc. Mex. Geól. Pet. 23, 1–112.
Carrillo-Bravo, J., 1982. Exploración Petrolera de la Cuenca Mesozoica del Centro de México. Bol. Asoc. Mex. Geól. Pet. XXXIV (1), 21–46.
Centeno-García, E., Silva-Romo, G., 1997. Petrogenesis and tectonic evolution of central Mexico during Triassic–Jurassic time. Rev. Mex. Cienc. Geol. 14 (2), 244–260.
Centeno-García, E., Ruiz, J., Coney, P.J., Parchet, P.J., Ortega-Gutiérrez, F., 1993. Guerrero terrane of Mexico: its role in the Southern Cordillera from new geochemical data. Geology 21, 419–422.
Christiansen, R.L., Lipman, P.W., 1966. Emplacement and thermal history of rhyolite lava flow near Fortymile Canyon, southern Nevada. Geol. Soc. Amer. Bull. 77, 671–684.
Christiansen, E.H., Bikun, J.V., Sheridan, M.F., Burt, D.M., 1984. Geochemical evolution of topaz rhyolites from the Thomas Range and Spor Mountain, Utah. Am. Mineral. 69, 223–236.
Christiansen, E.H., Sheridan, M.F., Burt, D.M., 1986. The geology and geochemistry of Cenozoic topaz rhyolites from the western United States. Geol. Soc. Am. 205, 82. Special Paper.
Cox, A., Dalrymple, G.B., 1967. Statistical analysis of geomagnetic reversal data and the precision of potassium–argon dating. J. Geophys. Res. 72, 2603–2614.
Damon, P.E., Shafiqullah, M., Clark, K.F., 1981. Age trends of igneous activity in relation to metallogenesis in the southern Cordilleran. Ariz. Geol. Soc. Dig. 14, 137–154.
Damon, P.E., Shafiqullah, M., Clark, K.F., 1983. Geochronology of the porphyry copper deposits and related mineralization in Mexico. Can. J. Earth Sci. 20, 1052–1071.
De Cserna, Z., 1956. Tectónica de la Sierra Madre Oriental de México, entre Torreón y Monterrey. Congreso Geológico Internacional 20, México, D.F., Monografía, p. 87.
Dickinson, W.R., Lawton, T.F., 2001. Carboniferous to Cretaceous assembly and Fragmentation of Mexico. Gol. Soc. Amer. Bull. 113, 1142–1160.
Ferrari, L., López-Martínez, M., Rosas-Elguera, J., 2002. Ignimbrite flare-up and deformation in the southern Sierra Madre Occidental, western Mexico—implications for the late subduction history of the Farallon Plate. Tectonics 21 (4). doi:10.1029/2001TC001302.
Ferrari, L., Valencia-Moreno, M., Bryan, S., 2005. Magmatismo y tectónica de la Sierra Madre Occidental y su relación con la evolución de la margen occidental de Norteamérica. Bol. Soc. Geol. Mex. LVII (3), 343–378.
Fink, J.H., 1987. The emplacement of silici domes and lava flows. Geol. Soc. Am. 212 Special Paper, 145 pp.
Fix, J.E., 1975. The crust and upper mantle of central Mexico. Geophys. J. R. Astron. Soc. 43, 453–499.
Foshag, W.F., Fries, C., 1942. Tin deposits of the Republic of Mexico. U.S. Geol. Surv. Bull. 935–C, 99–176.
Gill, J.B., 1981. Orogenic Andesites and Plate Tectonics. Springer–Verlag. 390 pp.
Henry, C.D., Price, G.J., 1984. Variation in caldera development in the Tertiary volcanic field of Trans-Pecos Texas. J. Geophy. Res. 89 (B-10), 8765–8768.
Henry, C.D., Aranda-Gómez, J.J., 1992. The real southern Basin and Range: mid-to late Cenozoic extension in Mexico. Geology 20, 701–704.
Hildreth, E.W., 1981. Gradients in silicic magma chambers: implications for lithospheric magmatism. J. Geophys. Res. 86 (B11), 10153–10192.
Huspeni, J.R., Kesler, S.E., Ruiz, J., Tuta, Z., Sutter, J.F., Jones, L.M., 1984. Petrology and geochemistry of rhyolites associated with tin mineralization in northern Mexico. Econ. Geol. 79, 87–105.
Labarthe-Hernández, G., Tristán-González, M., Aranda-Gómez, J.J., 1982. Revisión estratigráfica del Cenozoico de la parte central del Estado de San Luis Potosí. Instituto de Geología y Metalurgia, Universidad Autónoma de San Luis Potosí, Foll. Téc. 85, 208 p.
Labarthe-Hernández, G., Tristán-González, M., 1988. El domo La Negra y su ambiente tectónico en la Sierra de Encinillas Chihuahua. Instituto de Geología, Universidad Nacional Autónoma de México, Simposium sobre Geología Regional de México 3, Programa y Resúmenes, pp. 51–52.
Labarthe-Hernández, G., Aguillón Robles, A., Tristán-González, M., Jiménez-López, L.S., Romero, A., 1989. Cartografía geológica 1:50,000 de las Hoja El Refugio y Mineral El Rialito, Estados de San Luis Potosí y Guanajuato. Instituto de Geología, Universidad Autónoma de San Luis Potosí, Foll. Téc. 112, 76 p.
Labarthe-Hernández, G., Jiménez-López, L.S., 1991. Cartografía geológica 1:50,000 de las hojas Cerrito de Bernal, Santo Domingo, El Estribo y La Herradura, Estado de San Luis Potosí. Instituto de Geología, Univiversidad Autónoma de San Luis Potosí, Foll. Téc. 113, 62 p.
Labarthe-Hernández, G., Jiménez-López, L.S., 1992. Características físicas y estructura de lavas e ignimbrita riolíticas en la Sierra de San Miguelito, S.L.P. Instituto de Geología, Universidad Autónoma de San Luis Potosí, Foll. Téc. 114, 31 p.
Le Bass, M.J., Le Maitre, R.W., Streckeisen, A., Zanettin, B., 1986. A chemical classification of volcanic rocks based on the total alkali-silica diagram. J. Petrol. 27, 745–750.
Lee-Moreno, J.L., 1972. Geological and geochemical exploration characteristics of Mexican tin deposits in rhyolitic rocks. University of Arizona, Unpubl. PhD thesis, 180 p.
Lipman, P.W., 1984. The root of ash flow calderas in western North America—windows into the tops and granitic batholiths. J. Geophys. Res. 89 (B-10), 8801–8841.
López-Doncel, R., 2003. La Formación Tamabra del Cretácico en la porción central del margen occidental de la Plataforma Valles–San Luis Potosí, centro-noreste de México. Rev. Mex. Cienc. Geol. 20, 1–19.
Lozano, R., Bernal, J.P., 2005. Characterization of a new set of eight geochemical reference materials for XRF major and trace element analysis. Rev. Mex. Cienc. Geol. 22, 329–344.
McDowell, F.W., Clabaugh, S.E., 1979. Ignimbrites of the Sierra Madre Occidental and their relation to the tectonic history of western Mexico. Geol. Soc. Amer. 180, 113–124. Special Paper.
McDowell, F.W., Mauger, R.L., 1994. K–Ar and U–Pb zircon chronology of Late Cretaceus and Tertiary magmatism in Central Chihuahua State, Mexico. Geol. Soc. Am. Bull. 106, 118–132.
McDowell, F.W., Wark, D.A., Aguirre-Díaz, G.J., 1990. The Tertiary ignimbrite flare-up in western Mexico. Geol. Soc. Amer. 22 (26) Abstract with Programs.
McGehee, R.V., 1976. Las rocas metamórficas en el Arroyo La Pimienta, Zacatecas, Zacatecas. Bol. Soc. Geol. Mex. 37, 1–10.
Meyer, R.P., Steinhart, J.S., Woolard, G.P., 1958. Seismic determination of crustal structure in the central plateau of Mexico. Trans. Am. Geophys. Union 39, 403–413.
Middlemost, E.A.K., 1989. Iron oxidation ratios, norms and classification of volcanic rocks:. Chem. Geol. 77 (1), 19–26.
Morton, B.O., Hernández, E., Lounejeva, B.E., Armienta, M.A., 1997. Desarrollo y aplicación de un método analítico para la determinación de lantánidos en materiales geológicos por ICP-MS. Actas INAGEQ 3, 259–264.
Ngounouno, I., Déruelle, B., Demaiffe, D., 2000. Petrology of the bimodal Cenozoic volcanism of the Kapsiki plateau (northernmost Cameroon, Central Africa). J. Volcanol. Geotherm. Res. 103, 21–44.
Nieto-Samaniego, A.F., Macías-Romo, C., Alaniz-Alvarez, S.A., 1996. Nuevas edades isotópicas de la cubierta volcánica cenozoica de la parte meridional de la Mesa Central, Mexico. Rev. Mex. Cienc. Geol. 13, 117–122.
Nieto Samaniego, A.F., Ferrari, L., Alaniz Alvarez, S.A., Labarthe Hernández, G., Rosas Elguera, J., 1999. Variation of cenozoic extension and volcanism across the southern Sierra Madre Occidental volcanic province, Mexico. Geol. Soc. Am. Bull. 111, 347–363.
Nieto-Samaniego, A.F., Alaniz-Alvarez, S.A., Camprubí í Cano, A., 2005. La Mesa Central: estratigrafía, estructura y evolución tectónica cenozoica. Bol. Soc. Geol. Mex. 57 (3), 285–318.
Orozco-Esquivel, M.T., Nieto Samaniego, A.F., Alaniz Alvarez, S.A., 2002. Origin of rhyolitic lavas in the Mesa Central, Mexico, by crustal melting related to extension. J. Volcanol. Geotherm. Res. 118, 37–56.
Padilla y Sánchez, R.J., 1985. Las estructuras de la curvatura de Monterrey, estados de Coahuila, Nuevo Le'n, Zacatecas y San Luis Potosí. Inst. Geol., Univ. Nac. Autón. Méx. Revista 6, 1–20.
Peccerillo, A., Taylor, S.R., 1976. Geochemistry of Eocene calcalkaline volcanic rocks from the Kastamonu area, northern Turkey. Contrib. Mineral. Petrol. 58, 63–81.
Rivera, J., Ponce, L., 1986. Estructura de la corteza al oriente de la Sierra Madre Occidental, México, basada en la velocidad del grupo de las ondas Rayleigh. Geofís. Int. 25, 383–402.
Rock, N.M.S., 1987. The need for standardization of normalized multi-element diagrams in geochemistry: a comment. Geochem. J. 21, 75–84.
Rodríguez-Ríos, R., 1997. Caractérisation du magmatisme et des minéralisations associées du dôme de Pinos et des dômes de rhyolite à topaze du Champ Volcanique de San Luis Potosí (Mexique). Thèse de doctorat, Université Henri Poincaré Nancy-1 (France), 357 p.
Rodríguez-Ríos, R., Aguillón-Robles, A., Leroy, J.L., 2007. Evolución petrológica y geoquímica de un complejo de domos topacíferos en el Campo Volcánico de San Luis Potosí (México). Rev. Mex. Cienc. Geol. 24, 328–343.
Ruiz, J., Patchett, P.J., Arculus, R.J., 1988. Nd–Sr isotope composition of lower crustal xenoliths: evidence for the origin of mid-Tertiary felsic volcanics in Mexico. Contrib. Mineral. Petrol. 99, 36–43.
Ruiz, J., Patchett, P.J., Arculus, R.J., 1990. Reply to "Comments on Nd–Sr isotopic composition of lower crustal xenoliths: evidence for the origin of mid-Tertiary felsic volcanics in Mexico", by K.L. Cameron and J.V. Robinson. Contrib. Mineral. Petrol. 104, 615–618.
Schaaf, P., Heinrich, W., Besch, T., 1994. Composition and Sm–Nd isotopic data of the lower crust beneath San Luis Potosí, central Mexico: evidence from granulite-facies xenolite suit. Geochem. Geol. 118, 63–84.
Scheubell, F.R., Clark, K.F., Porter, E.W., 1988. Geology, tectonic environment, structural controls in the San Martin de Bolaños District, Jalisco. Econ. Geol. 83, 1703–1720.
Smith, L.D., Jones, R.L., 1979. In: Rieckers, R.E. (Ed.), Termal anomaly in Northern Mexico: An extensión of the Rio grande Rift(?), in Rio grande Rift: Tectonic and Magamatism. Am. Gephys. Union, pp. 269–278.
Steiger, R.H, Jäger, E., 1977. Subcommission on geochronology: convention on the use of decay constants in geo- and cosmochronology. Earth Planet. Sci. Lett. 36, 359–362.
Stewart, J.H., 1978. Basin-range structure in western North America — a review. Geol. Soc. Amer. Mem. 152, 1–31.
Stewart, J.H., 1998. Regional characteristics, tilt domains, and extensional history of the late Cenozoic Basin and Range province, western North America. Geol. Soc. Am. 323, 47–74. Special Paper.
Sun, S.S., McDonough, W.F., 1989. Chemical and isotopic systematics of oceanic basalts: implications for mantle composition and processes. In: Saunders, A.D., Norry, M.J. (Eds.), Magmatism in the Ocean Basins, vol. 42. Geol. Soc., pp. 313–345. Special Paper Publ.
Swanson, E.R., McDowell, F.W., 1984. Calderas of the Sierra Madre Occidental volcanic field western Mexico. J. Geophys. Res. 89, 8787–8799.
Tardy, M., Longoria, J.F., Martínez-Reyes, J., Mitre, L.M., Patillo, M., Padilla y Sánchez, R.J., Ramírez, C., 1975. Observaciones generales sobre la estructura la estructura de la

Sierra Madre Oriental: La aloctonía del conjunto Cadena Alta-Altiplano Central, entre Torreón, Coahuila y San Luis Potosí, S.L.P. México. Inst. Geol., Univ. Nac. Autón. Méx., Revista 75 (1), 1–11.

Torres-Hernández, J.R., Labarthe-Hernádez, G., Aguillón-Robles, A., Gómez-Anguiano, M., Mata-Segura, J.L., 2006. The pyroclastic dikes of the Tertiary San Luis Potosí volcanic field: Implications on the emplacement of Panalillo ignimbrite. Geofís. Int. 45, 243–253.

Tristán-González, M., 1986. Estratigrafía y tectónica del graben de Villa de Reyes en los estados de San Luis Potosí y Guanajuato, México. Inst. Geol., Univ. Autón. San Luis Potosí, Foll. Téc. 107, 91.

Tristán-González, M., 2008. Evolución tectono-magmática durante el Paleógeno en la porción sur-oriental de la Mesa Central. Tesis de Doctorado, Universidad Nacional Autónoma de México, Juriquilla, Qro. (México), 207 p.

Tristán-González, M., Torres-Hernández, J.R., Mata-Segura, J.L., 1994. Una deformación Pre-Laramídica, en la secuencia Vulcano-sedimentaria, de la parte oriental del Terreno Guerrero. GEOS 14, 82.

Tristán-González, M., Labarthe-Hernández, G., Aguillón-Robles, A., Aguirre-Díaz, G.J., 2005. Los domos exógenos del Oligoceno sin-extensionales de la Mesa Central: Características físicas. GEOS 25 (1), 203.

Tristán-González, M., Labarthe-Hernández, G., Aguillón-Robles, A., Torres-Hernández, J.R., Aguirre-Díaz, G., 2006. Diques piroclásticos en fallas de extensión alimentadores de ignimbritas en el occidente de Campo Volcánico del Río Santa María, S.L.P. GEOS 26 (163).

Tristán-González, M., Aguillón-Robles, A., Barboza-Gudiño, J.R., Torres-Hernández, J.R., Bellon, H., López-Doncel, R.A., Rodríguez-Ríos, R., Labarthe-Hernández, G., 2009a. Geocronología y distribución espacial del vulcanismo en el Campo Volcánico de San Luis Potosí. Bol. Soc. Geol. Mex. 61, 17–34.

Tristán-González, M., Aguirre-Díaz, G.J., Labarthe-Hernández, G., Torres-Hernández, J.J., Bellon, H., 2009b. Post-Laramide and pre-Basin and Range deformation and implications for Paleogene (55–25 Ma) volcanism in central Mexico: a geological basis for a volcano-tectonic stress model. Tectonophysics 471, 136–152. doi:10.1016/j.tecto.2008.12.021.

Verma, S.P., 1984. Sr and Nd isotopic evidence for petrogenesis of Mid-Tertiary felsic volcanism in the mineral district of Zacatecas, Zac. (Sierra Madre Occidental), Mexico. Isot. Geosc. 2 (1), 37–53.

Verma, S.P., Sotelo Rodríguez, Z.T., Torres Alvarado, I.S., 2002. SINCLAS: Standard Igneous Norm and Volcanic Rock Classification System. Comp. Geosc. 28 (5), 711–715.

Webster, D.J., Burt, D.M., Aguillón, R.A., 1996. Volatile and lithophile trace-element geochemistry of Mexican tin rhyolite magmas, deduced from melt inclusions. Geochem. Cosmochem. Acta 60 (17), 3267–3283.

Wilson, M., 1989. Igneous Petrogenesis: A global tectonic approach. Klumer Academic Publishers. 466 pp.

Yta, M., 1992. Etude geodynamique et metallogenique d'un sec Mexique La zone de Zacatecas-Francisco I Madero-Saucito.: L'Orleans, [Doctorate], dissertation, 48 p.